

Gulf of Mexico circulation within a high-resolution numerical simulation of the North Atlantic Ocean

Anastasia Romanou¹ and Eric P. Chassignet

Rosenstiel School of Marine and Atmospheric Sciences, Division of Meteorology and Physical Oceanography, University of Miami, Miami, Florida, USA

Wilton Sturges

Department of Oceanography, Florida State University, Tallahassee, Florida, USA

Received 7 January 2003; revised 27 August 2003; accepted 9 October 2003; published 3 January 2004.

[1] The Gulf of Mexico circulation is examined from the results of a high-resolution (1/12°) North Atlantic simulation using the Miami Isopycnic Coordinate Ocean Model. The motivation for this paper is twofold: first, we validate the model's performance in the Gulf of Mexico by comparing the model fields to past and recent observations, and second, given the good agreement with the observed Gulf of Mexico surface circulation and Loop Current variability, we expand the discussion and analysis of the model circulation to areas that have not been extensively observed/analyzed, such as the vertical structure of the Loop Current and associated eddies, especially the deep circulation below 1500 m. The interval between successive model eddy sheddings is 3 to 15 months, the eddy diameters range between 140 and 500 km, the life span is about 1 year, and the translational speeds are 2–3 km d⁻¹, in good agreement with observations. Areas of high cyclonic eddy occurrence in the model are southwest of Florida, the Loop Current boundary, and the western Campeche Bay area. The cyclonic eddy diameters range between 50 and 375 km, the orbital speeds range between 1 and 55 cm s⁻¹, the translational speeds range between 0.5 and 14 km d⁻¹, and the eddy life spans range between 1 and 3 months. The vertical structure of the temperature and salinity of each modeled eddy, from the moment it is shed until it disintegrates in the western Gulf of Mexico, is in agreement with the few available observations. Below 1500 m, deep cyclonic eddies are associated with the surface Loop Current anticyclones. The eddy variability is consistent with Rossby waves propagating westward, and there is bottom intensification of the flow close to steep topography. Overall, we show that this very high horizontal resolution isopycnic coordinate ocean model, which is able to produce a quite realistic surface circulation for the North and equatorial Atlantic, is also able to reproduce well the smaller-scale, basin-wide intricate dynamics such as the Gulf of Mexico variability.

INDEX TERMS: 4512 Oceanography: Physical: Currents; 4520 Oceanography: Physical: Eddies and mesoscale processes; 4532 Oceanography: Physical: General circulation; 4536 Oceanography: Physical: Hydrography; *KEYWORDS:* Gulf of Mexico, layer ocean modeling, Loop Current, eddies, deep circulation, energy conversions

Citation: Romanou, A., E. P. Chassignet, and W. Sturges (2004), Gulf of Mexico circulation within a high-resolution numerical simulation of the North Atlantic Ocean, *J. Geophys. Res.*, 109, C01003, doi:10.1029/2003JC001770.

1. Introduction

[2] Surface circulation features in the Gulf of Mexico, including the Loop Current, its rings, and the ring-shedding processes, have been well described through hydrographic observations, current meter and buoy measurements, satellite altimetry, and infrared imagery. The majority of the

observational studies deal with the Loop Current variability in the eastern gulf and with the anticyclonic eddy shedding frequency [Cochrane, 1969; Maul *et al.*, 1985; Sturges, 1992; Maul and Vukovich, 1993]. Recently, Bunge *et al.* [2002] have reported the results of a mooring experiment in the Yucatan Channel, showing the correlation of the deep transport across the Yucatan channel with the Loop Current extension, and thus with the eddy shedding. The periodicity of the eddy shedding process is one of the best known features of the Loop Current variability [Vukovich, 1988, 1995; Sturges, 1994; Sturges and Leben, 2000]. The westward propagation of eddies was examined by Elliott [1982]

¹Now at Courant Institute of Mathematical Sciences, New York University, New York, New York, USA.

and *Hamilton et al.* [1999]. Cold cyclonic perturbations that form around the Loop Current boundary were shown to be relevant to eddy shedding by *Vukovich* [1986, 1988]. *Fratantoni et al.* [1998] also observed large cyclonic eddies near the Dry Tortugas region and found that their evolution was correlated to the formation of anticyclonic Loop Current eddies.

[3] Beneath the Loop Current, there are very few observational studies of the circulation. *Molinari and Mayer* [1982] examined the bottom flow off Mobile, Alabama, and Tampa, Florida, and found that it was “more or less” aligned with the topography. *Hofmann and Worley’s* [1986] sections extend to the bottom, but the circulation patterns they describe depend on the choice of a level of no motion. *Hamilton* [1990] analyzed current meter measurements below 1000 m and found dominant low-frequency fluctuations (periods of 25 days and secondary spectrum peaks at 40 and 100 days) consistent with topographic Rossby waves. *Hamilton* suggested that the Loop Current and Loop Current eddies’ interactions with the topography in the northern gulf give rise to the fast moving topographic Rossby waves. *Hamilton and Fernandez* [2001] looked at deeper (2000 m) current meter measurements and found currents with speeds up to 100 cm s^{-1} in the northwestern gulf. These appeared to be decoupled from the currents above 1000 m and were associated with arrivals of Loop Current eddies in the area. Below 1500 m, the deep currents in the eastern gulf were depth-independent, with a tendency for bottom intensification and a 2-week period of variability.

[4] In contrast to the abundance of observational studies of some features like the Loop Current and associated eddies, there are only a few regional numerical simulations of the Gulf of Mexico circulation, such as those of *Hurlburt and Thompson* [1980], *Sturges et al.* [1993], *Oey* [1996], *Dietrich et al.* [1997], and *Welsh and Inoue* [2000]. Most of these studies include prescribed boundary conditions, i.e., specified inflow/outflow at the Yucatan Straits or farther south in the Caribbean basin. These restrictive boundary conditions preclude mesoscale variability other than that due to surface forcing, since they do not allow variability present outside the model domain to influence the Gulf of Mexico circulation. The need for boundary conditions far away from the Gulf of Mexico was first pointed out by *Sturges* [1992], who suggested that the plethora of spectral peaks in the eddy shedding spectrum was the result of frequency interactions, some of remote origin such as the North Brazil Current and the Gulf Stream. Consequently, *Sturges et al.* [1993] placed the outside model boundary at the Mid-Atlantic Ridge, and *Oey* [1996] demonstrated that setting the boundary farther south at the Caribbean rather than at the Yucatan Straits allowed for a better representation of the Gulf of Mexico circulation. *Ezer et al.* [2003] prescribed open boundaries sufficiently removed from the Gulf of Mexico to allow for a free dynamical interaction between the Caribbean Sea and the gulf through the Yucatan Channel.

[5] *Hurlburt and Thompson* [1980] performed a series of barotropic, reduced gravity, and two-layer sensitivity experiments on a $1/5^\circ$ horizontal grid, with no wind forcing, prescribed inflow across the Yucatan Straits, and idealized topography. Their model formed realistic eddies with shedding intervals of 8 months, but with unrealistic regularity

and strong sensitivity to the choice of horizontal eddy viscosity. They concluded that baroclinic instability is not the predominant eddy shedding mechanism, since they were able to achieve Loop Current shedding in both the two-layer and reduced gravity simulations.

[6] *Sturges et al.* [1993] used a $1/4^\circ$ horizontal grid for a larger domain (out to the Mid-Atlantic Ridge) with steady winds and produced a numerically quite realistic shedding frequency and shedding process, but with weak velocity fields. The deep flow was shown to be comprised of a family of cyclonic and anticyclonic eddies that were correlated, but not phase locked, with the surface Loop Current eddy. *Oey’s* [1996] numerical simulations ($1/5^\circ$ horizontal grid, realistic topography and river runoff, but only winter-time steady climatological forcing) showed a realistic eddy shedding frequency, but with rather weak and shallow anticyclones, strong correlation between the eddy shedding and a decrease or reversal of the deep transport at Yucatan, and bottom-intensified Rossby waves governing the dynamics in the deep western gulf.

[7] *Dietrich et al.* [1997], using a high horizontal resolution of $1/12^\circ$, 20 vertical levels, boundaries in the Caribbean, and winter forcing, found that cyclonic eddies in the western gulf were forced by the interaction of the Loop Current eddies with the topography; these eddies were sensitive to the horizontal viscosity choice. More recently, *Welsh and Inoue* [2000] used a model with $1/8^\circ$ horizontal resolution and 15 vertical levels, monthly mean wind stress, and seasonal boundary conditions at the Yucatan Straits. They found realistic surface circulation and pairs of cyclones-anticyclones in the deep layers.

[8] As already stated, one of the most common issues that have been addressed by the regional modeling studies is the impact of the placement of the open boundaries [*Sturges et al.*, 1993; *Ezer et al.*, 2003]. In this paper, we investigate in detail the Gulf of Mexico circulation from within a fine mesh ($1/12^\circ$) basin-scale North and equatorial Atlantic simulation performed with the Miami Isopycnic Coordinate Ocean Model (MICOM). In this model configuration, the circulation within the Gulf of Mexico is dynamically influenced by the large-scale flow variability present in the open Atlantic Ocean, such as the North Brazil Current, the Caribbean Sea circulation system, the Florida Current and the Gulf Stream. The motivation for this paper is twofold: first, the model’s performance in the Gulf of Mexico is validated by comparing the model fields to past and recent observations, and second, given the good agreement with the observed Gulf of Mexico surface circulation and Loop Current variability, the discussion and analysis of the model circulation is extended to areas that have not been extensively observed/analyzed such as the vertical structure of the Loop Current and associated eddies, especially the deep circulation below 1500 m.

[9] The paper is organized as follows: The numerical model configuration is described in section 2. In section 3, the model surface circulation is discussed with a focus on the Loop Current eddy formation and shedding and on the cyclonic eddies. This section aims to evaluate the model performance, since there is an abundance of observational and numerical references for the Gulf of Mexico surface circulation. In section 4, the model deep circulation is characterized and comparisons are made with observations

and other numerical studies wherever they exist. The transport through the Yucatan Straits, its vertical structure, and its variability are first described together with a brief discussion of the relation between the Loop Current eddy shedding and the deeper flow at the Straits. Then, the vertical structure of individual features such as the Loop Current eddies and the cyclonic eddies is discussed. The flow energetics at different levels are considered, in order to document possible mechanisms that are involved in the formation and separation of Loop Current eddies. The deep circulation (below 1500 m) is then described. Finally, some recapitulation and conclusions are offered in section 5.

2. Model Description and Configuration

[10] The Miami Isopycnic Coordinate Ocean Model (MICOM) is well documented in the literature. For a review, the reader is referred to *Bleck et al.* [1992] and *Bleck and Chassignet* [1994]. The fundamental reason for modeling ocean flow in density coordinates is that this system suppresses the diapycnal component of numerically caused dispersion of material and thermodynamic properties, such as temperature and salinity. This characteristic allows isopycnic models to prevent the warming of deep water masses, as has been shown to occur in models framed in Cartesian coordinates [*Chassignet et al.*, 1996]. Furthermore, the association of vertical shear with isopycnal packing and tilting in the ocean makes isopycnic models appropriate for studies of strong baroclinic western boundary currents such as the Yucatan and Florida currents and the Gulf Stream.

[11] The computational domain is the North and equatorial Atlantic Ocean basin from 28°S to 65°N, including the Caribbean Sea and the Gulf of Mexico. The horizontal grid (6 km on average) is defined on a Mercator projection with resolution $1/12^\circ \times 1/12^\circ \cos(\varphi)$, where φ is the latitude. The bottom topography is derived from a digital data set with 5' latitude-longitude resolution (ETOPO5). The vertical density structure is represented by 15 isopycnic layers, topped by an active bulk Kraus-Turner surface mixed layer that exchanges mass and properties with the isopycnic layers underneath. The vertical discretization was chosen to provide maximum resolution in the upper part of the ocean. Our relatively distant ocean boundaries at 28°S, 65°N, are treated as closed, but are bordered by 3° buffer zones in which temperature (T) and salinity (S) are linearly relaxed toward their seasonally varying climatological values [*Levitus*, 1982], with damping/relaxation time increasing from 5 days at the wall to 30 days at the inner edge of the buffer zone. These buffer zones restore the T and S fields to climatology in order to approximately recover the vertical shear of the currents through geostrophic adjustment. The surface boundary conditions are based on the Comprehensive Ocean-Atmosphere Data Set (COADS) mean monthly climatology [*da Silva et al.*, 1994]. The surface heat flux is prescribed using a linearized version of the bulk formulas [*da Silva et al.*, 1994] and the freshwater flux is a combination of observed E-P (i.e., COADS) and restoring to climatological surface salinity. The model was spun up from rest for a total of 20 years and the present analysis focuses on the final 5 years.

[12] The high horizontal grid resolution improves the model's behavior in comparison to that of previous coarse-resolution simulations. The major improvements are: (a) a correct Gulf Stream separation [*Chassignet and Garraffo*, 2001] and (b) higher eddy activity [*Paiva et al.*, 1999]. These results support the view that an inertial boundary layer, which results from the fine resolution, is an important factor in the separation process [*Özgökmen et al.*, 1997], and that resolution of the first Rossby radius of deformation is necessary for a correct representation of baroclinic instabilities.

[13] The model reproduces the most important characteristics of flow in the Caribbean. The total model transport through the Windward and Leeward Islands Passages into the Caribbean is 26.8 Sv, well within observational estimates of 18.4–33 Sv. The 5-year mean transport of 27.4 Sv through the Florida Straits is somewhat less than the canonical value of 30 Sv, with a seasonal cycle of the same magnitude and phase as seen in cable data [*Larsen*, 1992]. Model North Brazil Current rings provide most of the water for the Caribbean Throughflow (40%), and the model reproduces the three kinds of North Brazil Current rings observed to date [*Johns et al.*, 2003; *Garraffo et al.*, 2003]. The generation rate for the rings is 7–9 yr⁻¹, of which 6 are surface-intensified, in good agreement with observations from altimetry [*Goni and Johns*, 2001]. In addition, the model displays strong mesoscale variability in interisland passage transports with no clearly defined seasonality, consistent with what is known to date. The model eddy kinetic energy (EKE) in the Caribbean during the 5-year period averaged 800 cm²s⁻², ranging between 450 cm²s⁻² and 1250 cm²s⁻² [*Garraffo et al.*, 2001]; this agrees extremely well with results of a recent study by *Fratantoni* [2001], whose surface drifter-based calculations showed the Caribbean EKE ranging from 500 cm²s⁻²–1500 cm²s⁻². The behavior of numerical Lagrangian drifters and its comparison to that of real drifters is presented by *Garraffo et al.* [2001]. The probability density functions for the simulated Lagrangian data are discussed by *Bracco et al.* [2003]. Finally, *Paiva et al.* [1999] found that the length scales of the model eddy field compared favorably with altimeter-derived estimates.

3. Surface Circulation

[14] In this section, the model surface circulation in the Gulf of Mexico is described and compared to observations, focusing on the Loop Current and the formation and shedding of the large anticyclonic eddies and the cold core cyclonic eddies.

3.1. Loop Current and Shedding Process

[15] Figure 1 shows a sequence of the sea surface height every two months in the Gulf of Mexico for the 5-year analysis (model years 16–20). After entering the gulf through the Yucatan Straits, the Loop Current extends northwestward, occasionally shedding anticyclonic eddies known as Loop Current eddies (as in March and May of model year 17, September of year 18, March of year 19, and January of year 20). The Loop Current then exits the gulf through the Florida Straits and becomes the Florida Current.

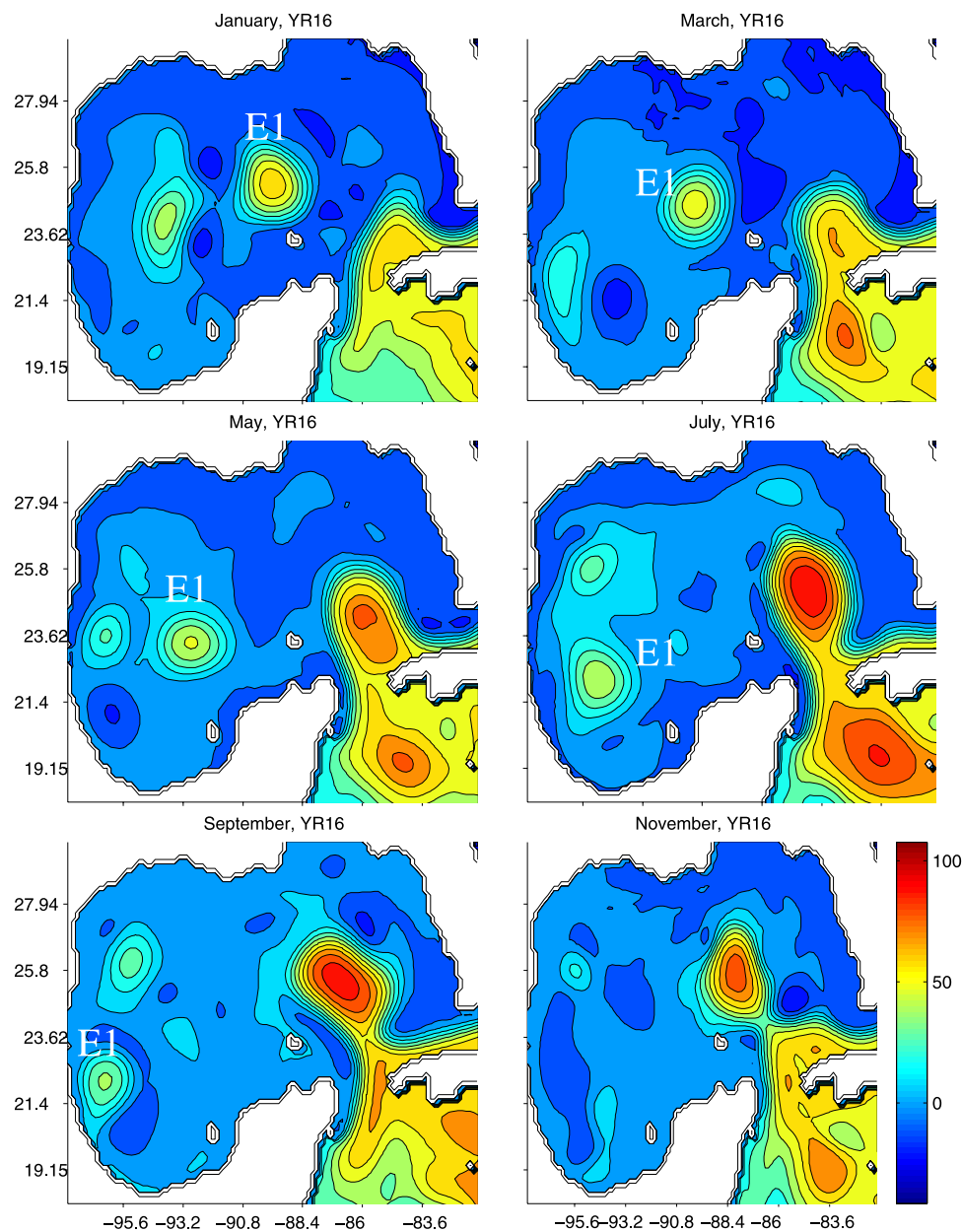


Figure 1. Model sea surface height (cm) every 2 months for the last 5 years of a 20-year model run. Color axis is common for all the frames and is shown next to the lower right frame. The x axis is longitude and the y axis latitude. Anticyclonic eddies that have pinched off the Loop Current are numbered as E(ddy)1-E6 and are described in Table 1.

[16] Once formed, the Loop Current eddies (or rings) travel westward and occasionally interact with previously formed warm-core eddies (as in July of year 16, July and September of year 17, and July of year 19). The rings sometimes interact with cyclonic eddies (as in March–May of year 16, November of year 17, March and November of year 19, and November of year 20). The larger anticyclonic rings also interact with the western boundary of the gulf (e.g., March–November of year 18 and September–November of year 20).

[17] Comparison with TOPEX/ERS satellite sea surface height data provided by the CCAR Real-time Altimeter Data Research Group (http://www-ccar.colorado.edu/~realtime/gom-real-time/_ssh/) shows that the model

Loop Current and Loop Current eddy evolution is realistic regarding the shape and path of the current and of the eddies, as well as the location of the low sea surface height anomalies. The maximum surface height in the modeled eddies is 60–90 cm, in good agreement with historical hydrographic data [Molinari and Morrison, 1988] as well as with the TOPEX/ERS satellite data. The sea surface height signature of the modeled cyclones is weak; the largest negative sea surface height anomaly in the model (–10 cm) is about 3 times weaker than that shown in the satellite data. It is likely that the small cold-core eddies (with diameters less than 10 km), which are the most energetic in the Gulf of Mexico, are not captured adequately with the present model resolution.

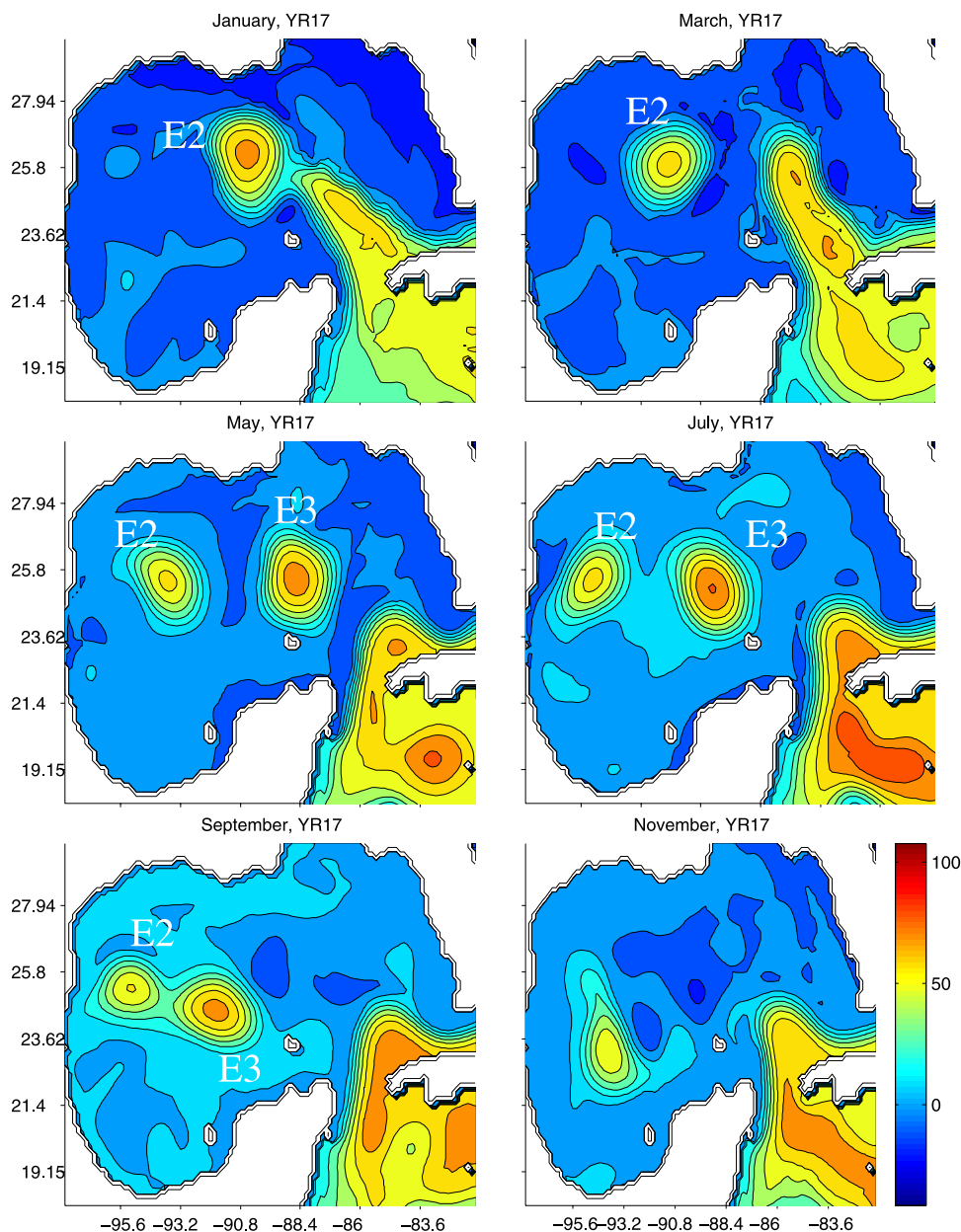


Figure 1. (continued)

[18] Figure 2 shows the northernmost latitude and the westernmost longitude of the Loop Current boundary, which are used here as surrogate variables for the Loop Current position (as by *Sturges* [1992]). The Loop Current boundary is defined as the line along which the Loop Current total kinetic energy drops below 35% of its maximum value at the center lobe of the Loop Current. The time series of the Loop Current position (Figure 2) shows that it typically extends northwestward within a 3° – 4° latitude range, in agreement with the results of *Maul and Vukovich* [1993, Figure 2]. The abrupt changes in the Loop Current position correspond to the times of shedding events. Usually, after a shedding event, the Loop Current retreats south to the Yucatan Straits (Figure 1: 16 January, 17 May, 19 March, and 20 January), though not always (Figure 1: 17 March and 18 September). The rate of change of the Loop Current position implies an average northward

displacement rate of 0.84 km d^{-1} and an average westward displacement rate of 0.86 km d^{-1} .

[19] Table 1 summarizes the characteristics of the model shedding activity in the 5-year period studied here. The first four columns show the dates and separation periods of all the events; the last four columns show the resulting eddy characteristics. In the model, the intervals between two subsequent shedding events range from 3 to 15 months, with an average of 8.8 months. These values agree well with those found in previous studies (Table 2), both from observations and from model results. The occurrence of multiple spectral peaks in the eddy shedding frequency was attributed by *Sturges* [1992] to interactions of the natural shedding frequency with the frequencies of variability of other oceanographic forcing fields, such as the Yucatan Channel inflow, the Florida Current and North Brazil Current variability, as well as the synoptic meteorological

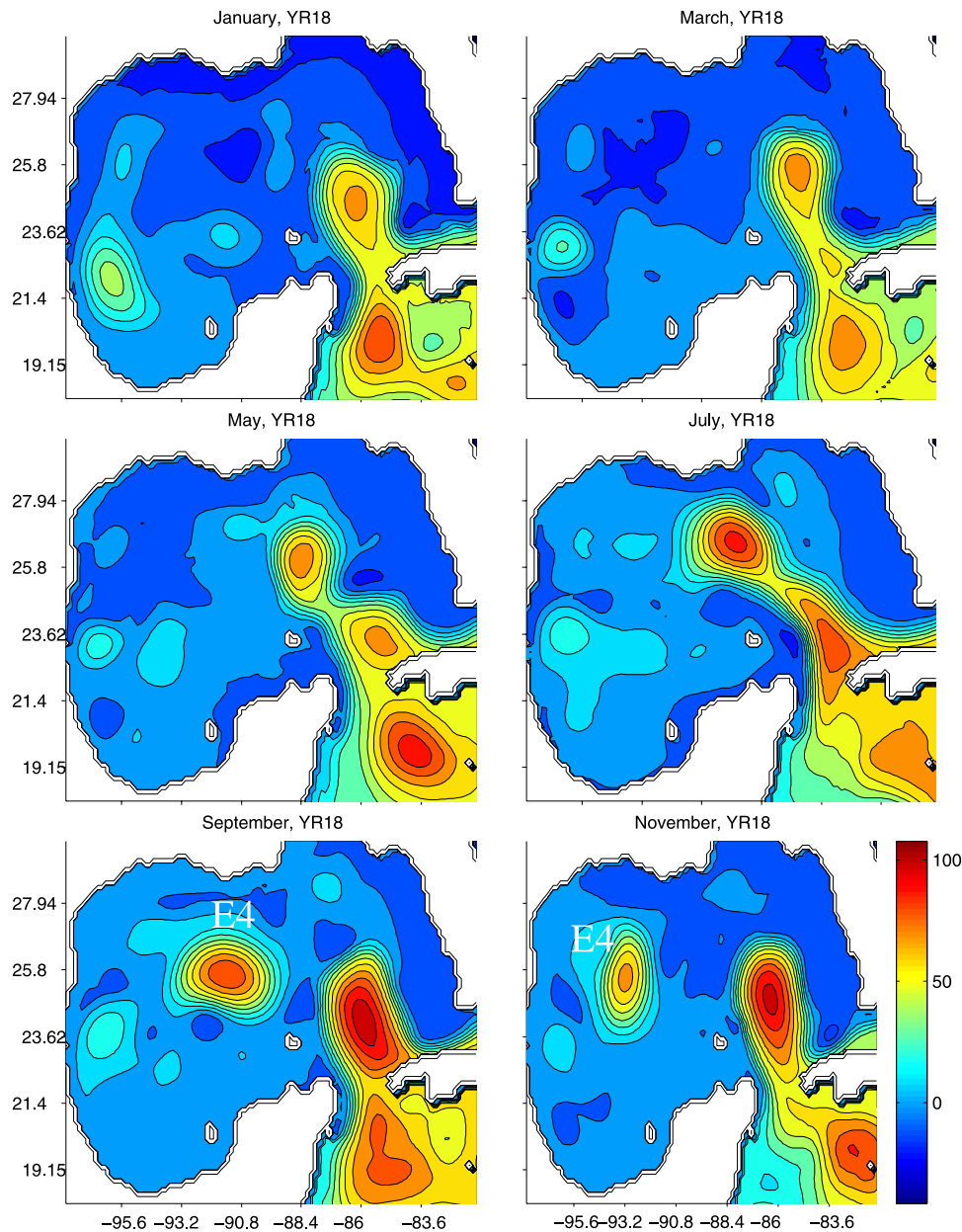


Figure 1. (continued)

forcing variability. These exact multiple frequency interactions explain why restricted model domains cannot capture adequately the Gulf of Mexico variability, since they exclude remotely imposed variability. In the present model, over a 5-year period, sheddings occur in various seasons: there are three sheddings in winter, one in spring, and one in summer. The Loop Current model eddies are not uniform in appearance and behavior. Their size ranges from 140 to 500 km and their life span from 10 to 17 months (with some occasional eddy merging prolonging their existence). For comparison purposes, Table 2 summarizes the results from observations and previous numerical studies. The shedding interval varies between 6 to 11 months in observations and between 4 to 17 months in other numerical studies (Table 2).

[20] The model eddy translational speeds range from 2.3 to 3.2 km d⁻¹ (Table 1), similar to the observed speeds by *Cochrane* [1969], *Elliott* [1982], and *Hamilton et al.* [1999]

(Table 2). The model eddy propagation speeds agree well also with the theoretical estimates of *Cushman-Rosin et al.* [1990], which show that, on average, an isolated eddy should propagate westward at the long Rossby wave speed βR_d^2 . Using characteristic values for the eddy parameters ($R_d = \sqrt{g'h}/f = 40$ km, with $g' = 0.03$ m s⁻¹ and h = the depth of the eddy ≈ 400 m), the long Rossby wave speed in the Gulf of Mexico is approximately 2.7 km d⁻¹.

[21] The maximum eddy orbital speeds are generally between 150 and 190 cm s⁻¹ with a mean of 170 cm s⁻¹. The orbital speeds are usually stronger in the newly formed eddies and decrease as the eddies move toward the west. *Hamilton et al.* [1999] observations show much weaker orbital speeds than in the rings modeled in this study (Table 1) and in other numerical simulations (Table 2). However, and as it will be shown next, orbital speeds vary greatly with the distance from the center of the eddy, and a

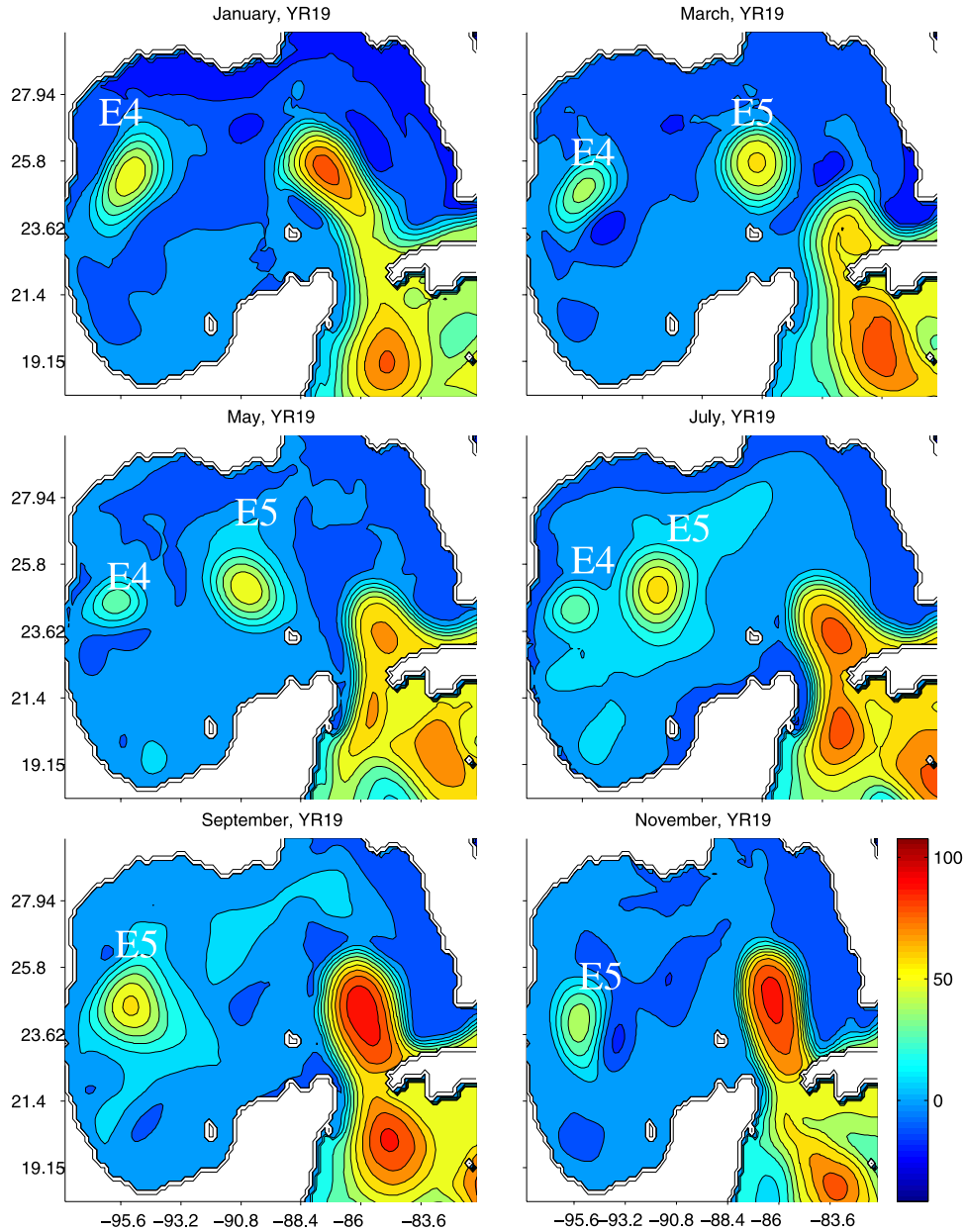


Figure 1. (continued)

meaningful comparison between the orbital speeds can only be made at similar distances from the eddy center.

[22] Model simulations of eddies provide an opportunity of describing eddy characteristics that are difficult to measure in situ. The functional form of the azimuthally averaged surface speed of newly formed and of mature eddies is shown in Figure 3. In all the eddies examined here, the speed is linearly increasing from about $10\text{--}20\text{ cm s}^{-1}$ at the center of the eddy to $60\text{--}110\text{ cm s}^{-1}$ at $92\text{--}100\text{ km}$ away from the eddy center. From the point of this maximum speed out toward the outer edge of the ring, the speed decreases exponentially. Younger eddies which are also the largest ones, are the most vigorous, while older eddies that have advanced farther west in the Gulf of Mexico have reduced maximum speeds with the location of the maximum speed at $60\text{--}70\text{ km}$ from the eddy center. Linear least squares fitting to the data for distances up to 95 km from

the eddy core, and exponential regression fitting for the rest of the data out toward the edge of the ring, yield the functional form of the azimuthally averaged speed:

$$\overline{u(r)} = \begin{cases} 8.45 \times 10^{-6}r + 1.23 \times 10^{-4} & : r \leq 92.5\text{ km} \\ 1.96 \times 10^{-4} - 845.4e^{-0.11r} + 8.66re^{-0.11r} & : r > 92.5\text{ km} \end{cases} \quad (1)$$

where, $\overline{u(r)}$ is in km s^{-1} and r is in km .

[23] From equation (1), one may deduce useful properties of the eddy such as the eddy rotational period $P_{\text{eddy}} = \frac{2\pi r}{\overline{u(r)}}$, where r is the distance from the eddy center and $\overline{u(r)}$ is the azimuthally averaged speed at distance r . Here, the eddy rotation periods vary from about 4 days near the center of the eddy, to 11 days at about 100 km from the

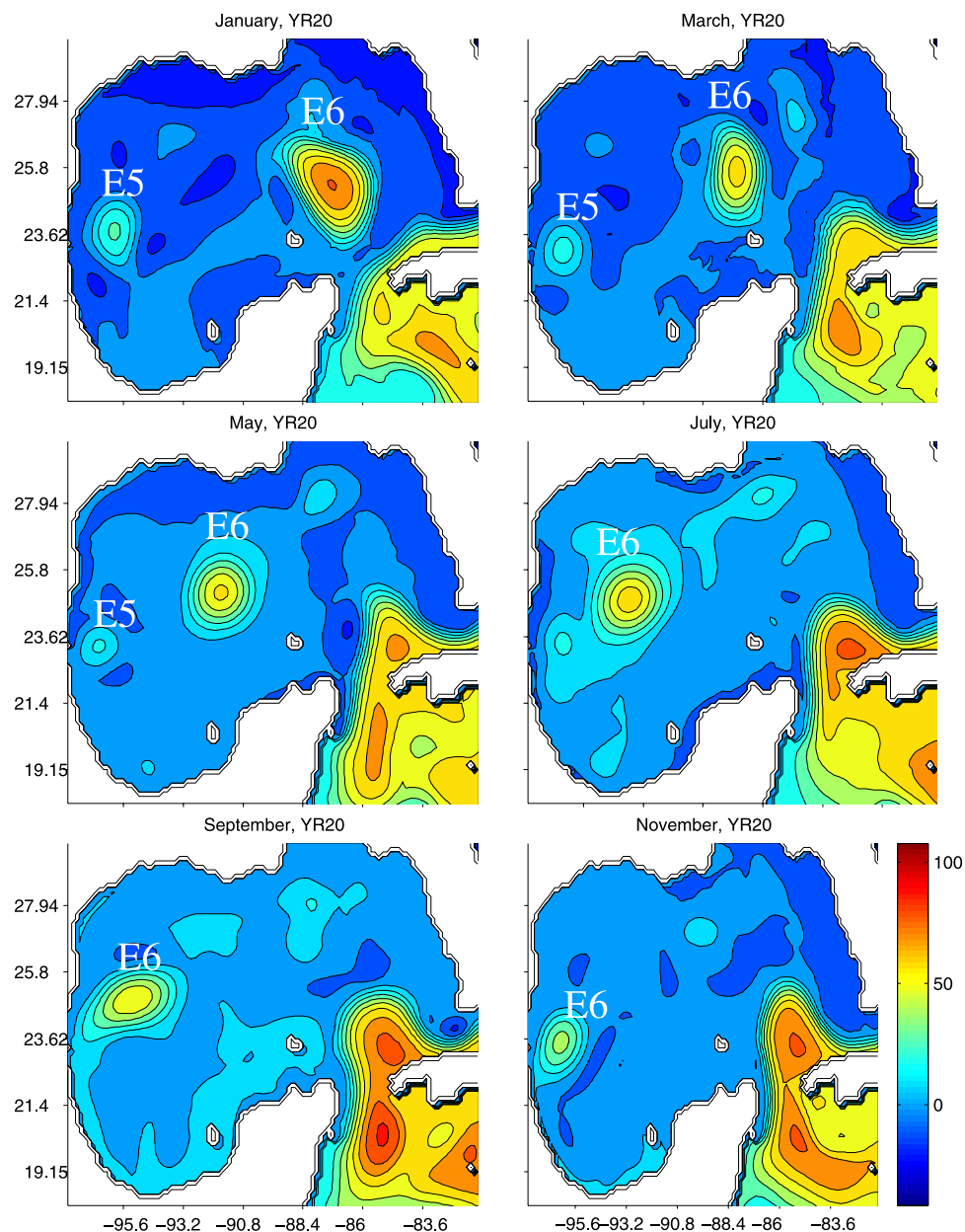


Figure 1. (continued)

center and 100 days at 200 km from the center of the eddy. Kinematic analysis of buoy drifters [Hamilton *et al.*, 1999] showed similar results; the rotation periods of the Loop Current anticyclones increase in time and, range between 6–20 days. Since buoys are usually trapped in the more vigorous part of the flow, i.e., near the maximum velocities, such periods agree well with the 4–11-day periods found in the model.

[24] The paths of the eddy centers (Figure 4) compare well with observations by Elliott [1982] and Hamilton *et al.* [1999, Figure 9] and with the results of numerical simulations by Oey [1996, Figure 12]. The eddies form over level topography 3000–3500 m deep, within a wide area (87° – 91° W and 21.8° – 25° N), then “sprint” over the plateau in the central-western Gulf of Mexico, following no particular pathway. Some eddies travel along the northwestern gulf continental slope while others cross the midwestern

gulf plateau. The eddies “stall” when they reach a topographic gradient and disintegrate within 95.5° – 97° W and 25.4° – 26.4° N, above the steep slopes of the Texas coast between 2000 and 3000 m depth. Two distinct eddy “graveyards” are detected at 23.6° N and at 22.1° N.

3.2. Cyclonic, or Cold-Core, Eddies

[25] Several cyclonic eddies have been observed to form in the Gulf of Mexico [Vukovich, 1986, 1988; Fratantoni *et al.*, 1998], but have not been studied as extensively as the warm-core anticyclones. The cyclones are often found to be associated with Loop Current boundary variations [Vukovich and Maul, 1985] and travel clockwise around the Loop Current. Westward propagation of some of these eddies is associated with the Loop Current warm-core eddy formation and shedding [Cochrane, 1969]. Some cyclones are known to reach the Straits of Florida area, giving rise to

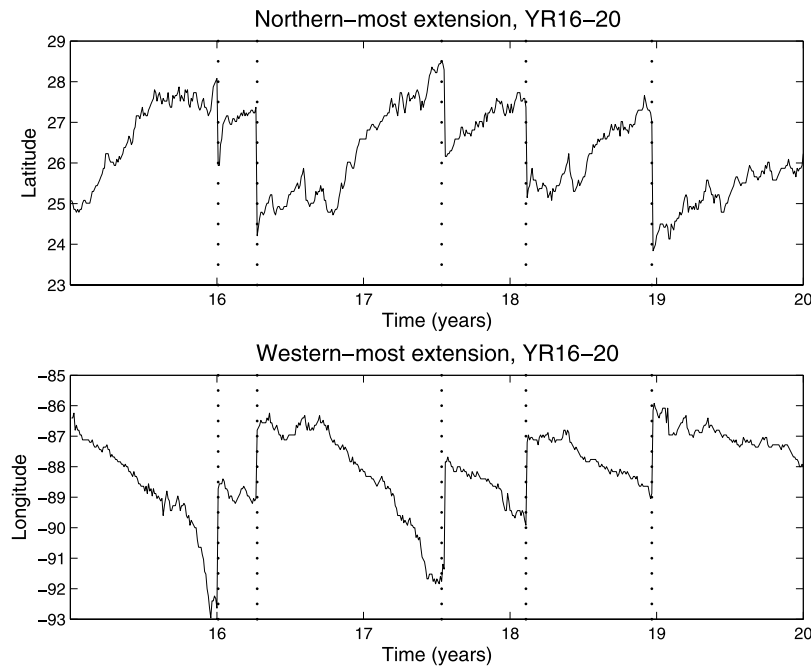


Figure 2. (a) Northernmost extension and (b) westernmost extension of the Loop Current boundary versus time for the last 5 years of a 20-year model run. The dotted lines correspond to eddy shedding events and correspond to eddies labeled E2–E6 in Figure 1 and Table 1.

a semipermanent cyclone in the Dry Tortugas region [Lee *et al.*, 1995] and later squeezing through the Florida Straits [Fratantoni *et al.*, 1998]. Cyclonic eddies are also evident in numerical simulations, as by Oey [1996], who found cyclonic eddies off southwestern Florida, and by Dietrich *et al.* [1997], who associated them with the Loop Current boundary variations. The cyclonic eddies by Oey [1996] did not contribute to the ring shedding process, but the eddies were nonetheless energized during the shedding period.

[26] In the present model, there are several cyclonic eddies present at any time in the gulf (Figure 1), predominantly around the Loop Current and Loop Current eddy boundaries (e.g., January and September of year 16, September of year 18, January and September of year 19, and January of year 20). At times, they are also found in the area between southern Florida and Cuba (as in May and November of year 16, March and November of year 18, and September of year 20) and occasionally close to the western gulf coast due to the interaction of the Loop Current eddies with the western gulf topography (November of year 16 and March and November of year 18).

[27] The occurrence density of modeled cyclones is illustrated in Figure 5. Most frequently, cyclones are found off the southern tip of Florida. In the model they are either generated locally or end up there after moving cyclonically around the Loop Current boundary. Cyclones are also generated over the shelfbreak region of the Campeche Bank. The rest model cyclones are encountered away from the shelf region and are either associated with Loop Current boundary undulations or eddy-eddy interactions (Figure 1). The formation of cyclones in the western gulf of Mexico appears to be correlated with large topographic gradient and the arrival of Loop Current anticyclones.

[28] The diameters of the model cyclones average 170 km, their orbital speeds 8 cm s^{-1} , and their translational speeds

2.3 km d^{-1} , in agreement with observed values (Table 3). Often, especially northwest of the Campeche Peninsula, cyclonic filaments extend into the central gulf and eventually form cyclonic eddies. The strongest eddies are found in the model off the western Louisiana-Texas (LATEX) shelf region (surface signature of 50 cm s^{-1}), southwest of Florida (up to 30 cm s^{-1}), and off the eastern Campeche Peninsula (30 cm s^{-1}). The range of the cyclonic eddy lifetimes varies considerably. In the Campeche Bay area, eddies live for 2 to 6 months (Figure 1: as in March–May of year 16, March–May of year 18, and November of year 19 to May of year 20). Southwest of Florida, the eddies do not live as long (1 to 3 months), and they usually exit the Gulf of Mexico through the Florida Straits.

4. Vertical Structure and Deep Circulation

[29] In the previous section, the numerical model was shown to be able to well reproduce the Loop Current variability and the eddy shedding process in the Gulf of Mexico. It was also shown that the Loop Current eddies that are formed have realistic surface signatures and that the cyclonic activity is close to that observed. In contrast to the surface circulation in the Gulf of Mexico, the flow at depth

Table 1. Synopsis of the Loop Current Eddy Characteristics Based on the Last 5 Years of the Present Model Run

eddy	Month	Year	Shedding Interval, months	Translation Speed, km d^{-1}	Orbital Speed, cm s^{-1}	Size, km	Life Span, months
1				3.2 ± 1.2	—	320–160	11+
2	Jan.	17		3.1 ± 1.8	150	400–220	10
3	Apr	17	3	2.4 ± 1.6	180	420–150	16
4	Jul	18	15	2.9 ± 1.5	160	420–140	12
5	Feb.	19	7	2.3 ± 1.5	190	400–140	17
6	Dec.	19	10	2.6 ± 1.5	160	500–150	12+

Table 2. Loop Current Eddy Characteristics From Observations and Other Numerical Model Results^a

	Shedding Interval, months	Translation Speed, km d ⁻¹	Orbital Speed cm s ⁻¹	Size, km	Life Span, months
<i>Cochrane</i> [1969]		2.5			
<i>Elliott</i> [1982]		2.1		366	12
<i>Vukovich</i> [1988]	11 (6–17)				
<i>Maul and Vukovich</i> [1993], <i>Hamilton et al.</i> [1999]		3.6 ± 4.7 ^b 1.72 ± 4.9 ^c	46.8 ± 12.8 ^b 36 ± 8.1 ^c	130 ± 34 ^b 102 ± 24 ^c	
<i>Maul et al.</i> [1985], <i>Sturges</i> [1992], <i>Sturges</i> [1993], <i>Vukovich</i> [1995]	8–9				
<i>Sturges and Leben</i> [2000]	6 and 11 (9)				
<i>Hurlburt and Thompson</i> [1980]	9.5		160–500		
<i>Sturges et al.</i> [1993]	7	4.4	70		
<i>Oey</i> [1996]	6.5–17	3–5	65	200–400	3.5–7
<i>Welsh and Inoue</i> [2000]		4	<100		12
<i>Ezer et al.</i> [2003]	4.2–10.9				

^aFirst 10 rows refer to observations, and the last 5 refer to models. Further information about each is given in section 1.1.

^bEastern gulf.

^cWestern gulf.

is only known through fragmented observations and scarce numerical simulations. In this section, we expand the model analysis to discuss the vertical structure of the Loop Current and associated eddies as well as the deep circulation below 1500 m.

4.1. Vertical Structure of the Flow Across the Yucatan Straits

[30] In the model, the mean transport across the Yucatan Straits is 27 Sv (Figure 6), with values ranging between 18 and 32 Sv. This is in agreement with several observations

(as quoted from Table 1 of *Sturges and Hong* [2000]: 29.9 Sv ± 3.7 Sv; *Sheinbaum et al.* [2002]: 23.8 Sv ± 1 Sv, with choices made in regional numerical simulations (*Hurlburt and Thompson* [1980], 30 Sv; *Oey* [1996], 30 Sv; and *Welsh and Inoue* [2000], 28 Sv), and with the results of *Ezer et al.* [2003] 25.3 ± 3.2 Sv).

[31] *Hurlburt and Thompson* [1980] were able to numerically simulate a Loop Current eddy shedding with a constant inflow of 30 Sv prescribed across the Yucatan Straits, thus disassociating (in their model) the variability of the inflow at Yucatan from the shedding frequency. How-

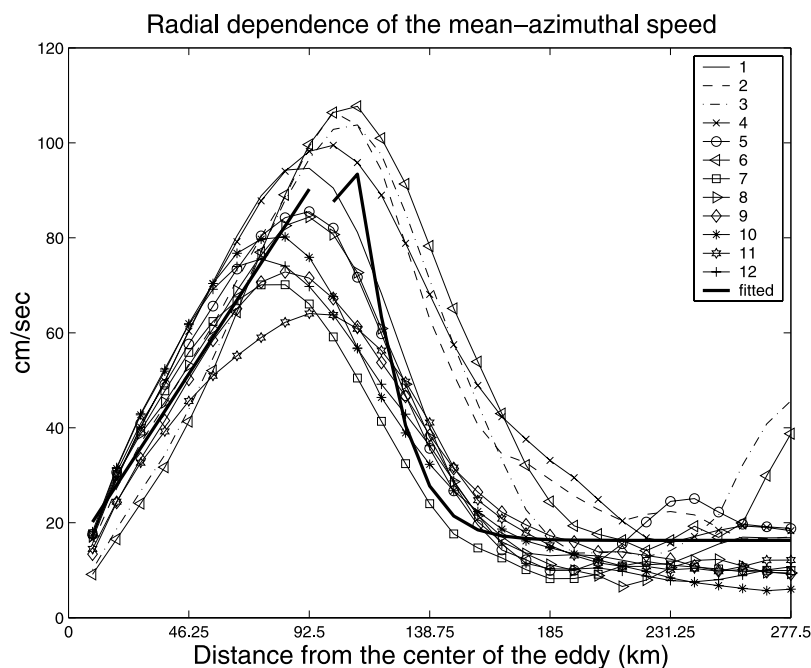


Figure 3. Azimuthally averaged eddy speed for all Loop Current eddies shed during the 5 years of model run. The first six eddies are recently shed and correspond to 1 (E1-Jan16), 2 (E2-Jan17), 3 (E3-May17), 4 (E4-Sept18), 5 (E5-Mar19), and 6 (E6-Jan20) in Figure 1. The last seven eddies are mature eddies and correspond to 7 (E1-May16), 8 (E2-May17), 9 (E2 + E3-Nov17), 10 (E4-Jan19), 11 (E5-Sept19), and 12 (E6-Jul20) in Figure 1. The thick solid line represents the linear polynomial fitting for the first part of the data and linear regression fitting for the second part.

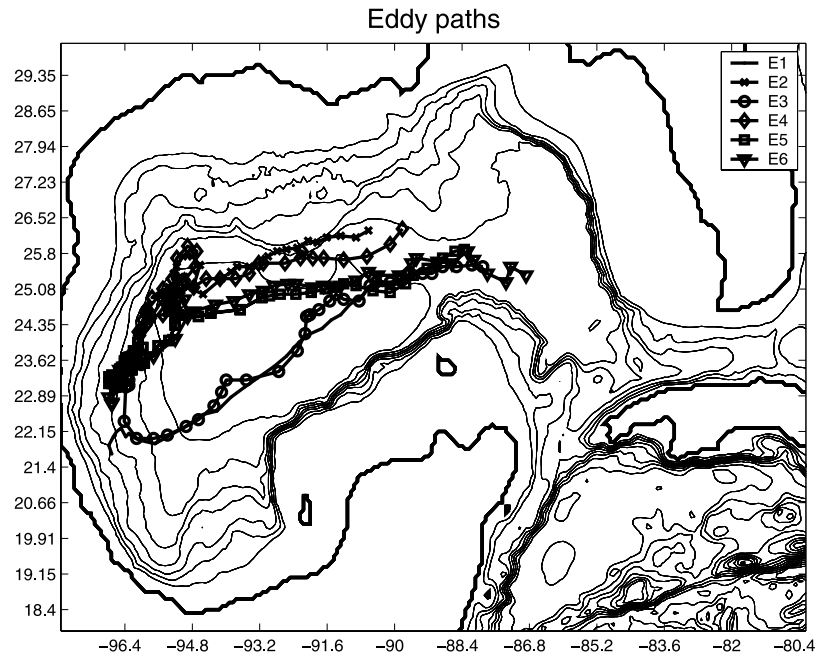


Figure 4. Paths of the Loop Current eddies referenced in Table 1 and during the 5 model year record studied here. Dots are at 9-day intervals, and depth contours are every 500 m. The eddy numbers correspond to eddies E1–E6 in Figure 1.

ever, in their results there was no variability in the eddy-shedding period or in the amplitude of the northernmost extension of the Loop Current into the Gulf of Mexico, contrary to what has been observed (see discussion in section 3.1). Moreover, recent studies, such as those of *Pichevin and Nof* [1997], suggest that the frequency of eddy shedding should be a function of transport.

[32] Figure 7 shows the model transport in the upper as well as in the lower layers. The upper layer (i.e., the first 11

model isopycnic layers) extends to 970 m and the deeper layer (i.e., isopycnic layers 12–14) extends to 2000 m. Wherever topography is shallower than those depths, the layers become massless. Layers 15 and 16 (which correspond to depths greater than 2000 m) are always massless across the Yucatan Channel. Ring shedding events are denoted with dotted lines.

[33] The model total transport exhibits large variability that is remarkably consistent with the findings of *Bunge et*

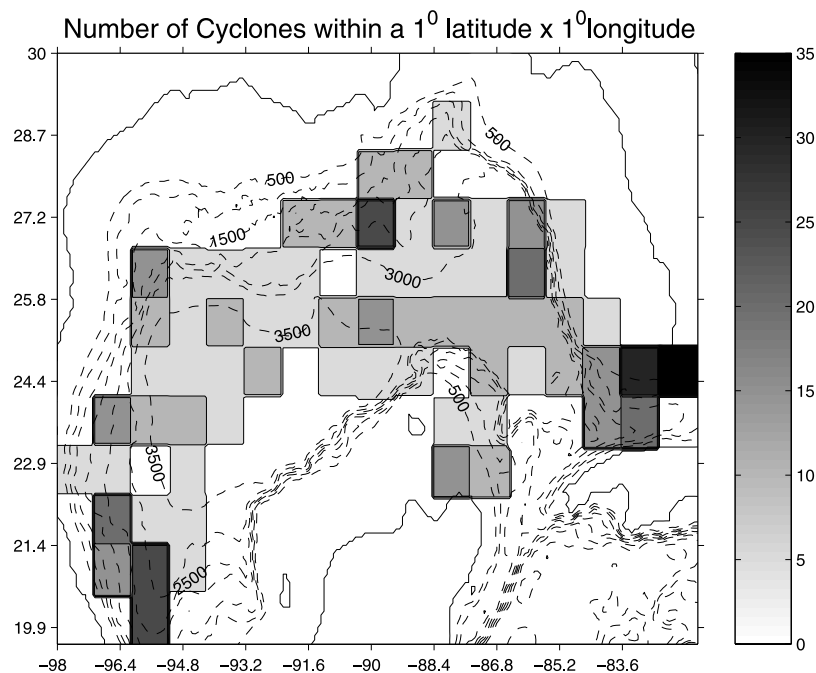


Figure 5. Number of model cyclones occurring in $1^\circ \times 1^\circ$ boxes over the 5 model year record studied here, based on Figure 1. Topography is also shown at 500 m contour interval.

Table 3. Cyclonic Eddy Characteristics From the Present Model and Two Sets of Observations

	Diameter, km	Translational Speed, km d ⁻¹	Orbital Speed cm s ⁻¹ ,	Life Span, months
Present model	50–375	0.5–14	1–55	1–6
Vukovich and Maul [1985]	80–120	4–10	20–100	
Vukovich [1988]	100–250	4–10		

al. [2002]. There is a spectral peak at 10 months and also at 6 and 2 months in the total transport. Maul *et al.* [1985] measurements showed that most of the variability occurs at 7, 4, and 1 months, while Ezer *et al.* [2003] simulations point to 11, 7, and 2 months. It is interesting that although the Ezer *et al.* [2003] wind-forcing field contains higher temporal resolution (6 hourly) than that of the present model (monthly mean), the variability of the flow through Yucatan is essentially the same, implying that the intramonthly wind variability does not play a role in the Yucatan Straits throughflow variability. Most of the model transport across the Yucatan Straits is confined to the upper 900 m (Figure 7). The correlation between the location of the northernmost extension of the Loop Current and the upper transport is low (0.4).

[34] Several studies have investigated the correlation between the surface flow through the Yucatan Straits and the flow below the depth sill. In this work as well as in previous numerical studies by Hurlburt and Thompson [1980] and Oey [1996], the upper and lower layer flows are anticorrelated (correlation coefficient -0.6), with the lower layer transport (Figure 7) being southward 60% of the time (i.e., exiting the Gulf of Mexico). The mean transport below 900 m (lower curve in Figure 14) is -0.07 Sv; the variability is large, from -2 to $+4$ Sv, with a standard deviation of 1.3 Sv. Observations by Maul *et al.* [1985] did not find any significant correlation between the eddy shedding process and the deep flow in the Yucatan Straits. However, their 3-year-long data record came from a pair of current meters closely spaced together and moored at the middistance between Cuba and Yucatan at 145 m above the sill, and thus may not be representative of the total throughflow.

[35] Relating the deep Yucatan throughflow to the Loop Current variability and the eddy shedding process has been the focal point of several investigations. Oey's [1996] simulations suggested that southward flow in the Yucatan Straits preceded a shedding event. More recently, the Bunge *et al.* [2002, Figure 3] mooring study showed that the flow in the deeper layer becomes southward across the Yucatan Straits when the area inside the Loop Current increases before a shedding event. The present model simulation exhibits a similar behavior with the deep flow decreasing in the months preceding an eddy shedding (while the Loop Current penetrates northward and its area increases) (Figure 7b) and becoming southward in 4 out of 5 Loop Current eddy sheddings.

[36] Figure 8 shows the mean pattern of the meridional velocity across the Yucatan Straits. We find a near-surface, $2\text{--}8$ cm s⁻¹ southerly flow confined to the Cuban side, up to 1 cm s⁻¹ outflow in the western wall of the straits, and inflow in the deep middle section of the straits. Here, the model shows little mean flow in the range of 800 to 1000 m,

although the variance there is large (Figure 9), implying strong eddy activity. Maul *et al.* [1985] found deep flow (just above the sill) that was southward, and occasional northward flow (around 5 cm s⁻¹), over periods lasting from a few days to 3 months. It is possible that their mooring results are contaminated by midchannel trapped eddies. However, findings here are in very good agreement with those of other modeling studies [Ezer *et al.*, 2003, Figure 4].

4.2. Vertical Structure of the Loop Current Eddies

[37] The vertical structure of the modeled Loop Current eddies is in good agreement with observations by Cochrane [1969] and Elliott [1982], and with the results of other model simulations by Welsh and Inoue [2000]. Here, the temperature in the center of recently shed eddies ranges from 17 to 22°C at 200 m. The surface salinity ranges from 36 to 36.4 ppt with a subsurface maximum of 36.6 ppt at ~ 200 m (Figure 10). As by Elliott [1982], the modeled Loop Current eddies are characterized by the Loop Current water, i.e., the Caribbean Subtropical Underwater, which has high salinity (36.6 ppt) on the 22.5°C isotherm, differing from the surrounding Gulf of Mexico waters which have salinity 36.4 ppt on the same isotherm. Early in their existence, the modeled eddies show nearly constant temperature and salinity gradients of about $0.06^\circ\text{C m}^{-1}$ and 0.01 ppt m⁻¹, respectively, between 150 and 300 m. These gradients express the model-evolved vertical T,S structure in the Gulf of Mexico with relaxation boundary conditions applied only at 28°S and 65°N (see section 2). The minimum salinity of 34.7 ppt at 400 m is associated with the Antarctic Intermediate Water.

[38] Vukovich and Crissman [1986, Figure 2b] presented a transect through a wintertime eddy (shed in January). The

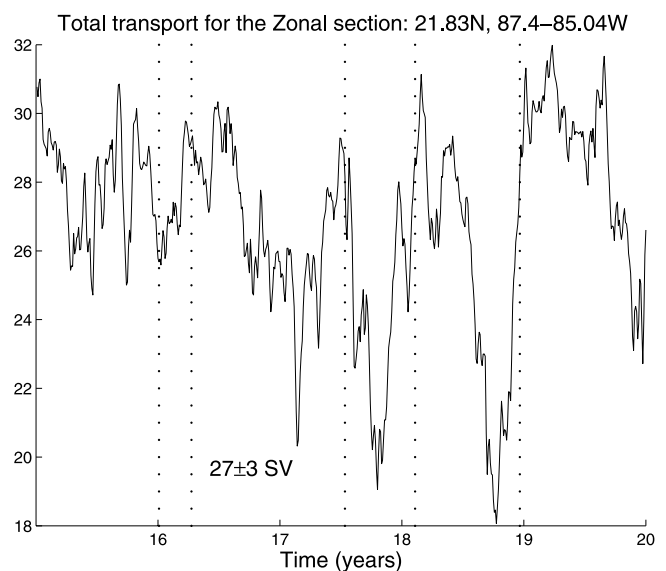


Figure 6. Total transport across the Yucatan Straits (21.83°N , $87.44^\circ\text{--}85.04^\circ\text{W}$) during the last 5 years of a 20 year model run. The dotted lines correspond to eddy-shedding events and correspond to eddies labeled E2–E6 in Figure 1 and Table 1. The mean and standard deviation of the transport is 27 ± 3 Sv.

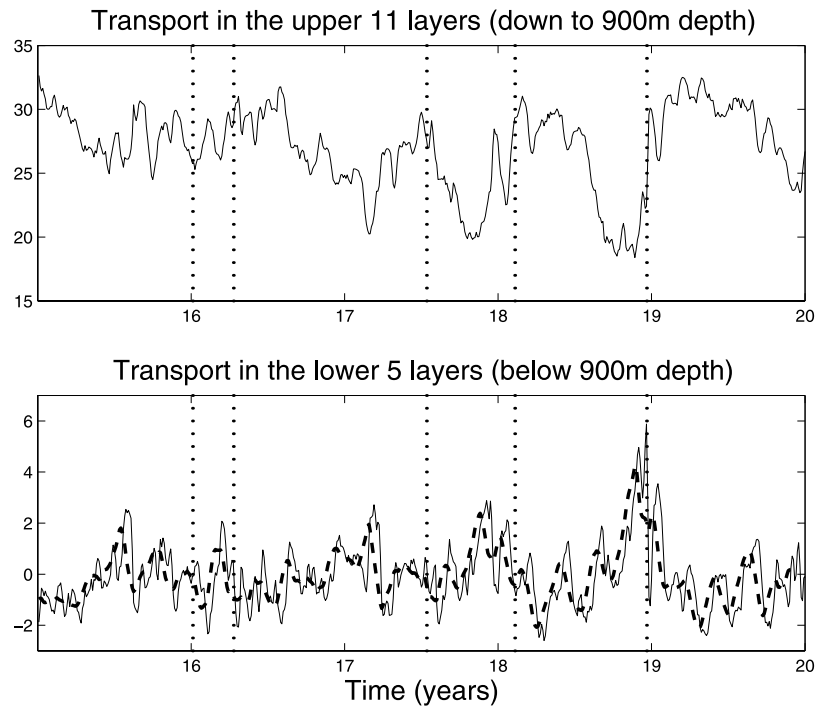


Figure 7. (top) Layer transport across the Yucatan Straits (21.83°N , $87.44^{\circ}\text{--}85.04^{\circ}\text{W}$) in the upper 11 layers, which extend to 900 m depth (upper panel), and in the lower five layers. (bottom) The dashed line is the 30-day running mean of the deep transport. The dotted lines represent times of eddy shedding corresponding to E2–E6 in Figure 1 and Table 1. The horizontal axis is time for the years 16–20 of the model run.

depth of the 20°C isotherm was 90–200 m, while in the model (January eddies: E1 and E2) that depth is also 100–200 m (Figure 10). The 10°C isotherm is shallower in the model (at 450 m) than in the observations (500–580 m).

[39] Comparison between summertime eddies [Elliott, 1982, Figure 1] and E3 from the model (Figure 10) shows that although the model surface temperature is slightly warmer than that in the observations, the depth of the 20°

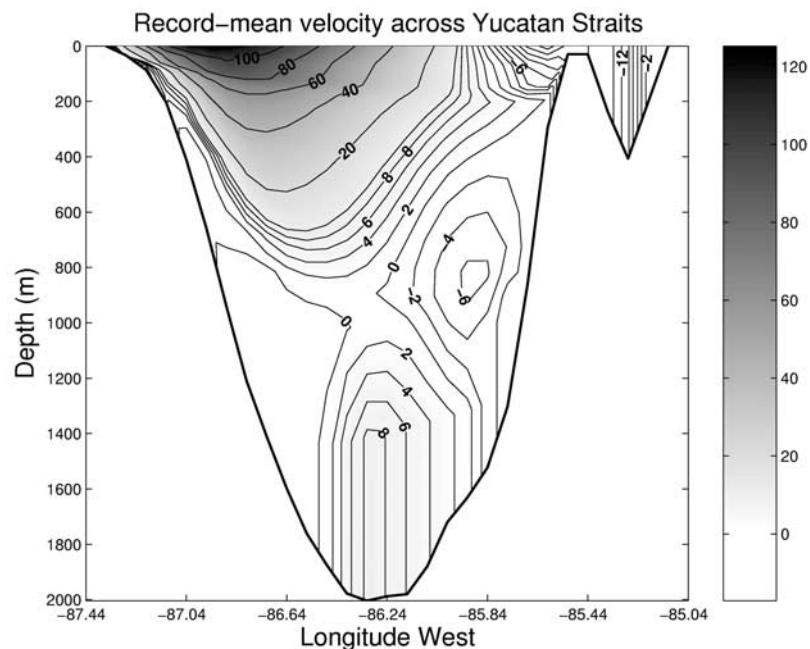


Figure 8. Mean meridional velocity (in cm s^{-1}) across the Yucatan Straits. The mean is taken over the 5 years of the model run studied here and at 21.83°N and $87.4^{\circ}\text{--}85.04^{\circ}\text{W}$.

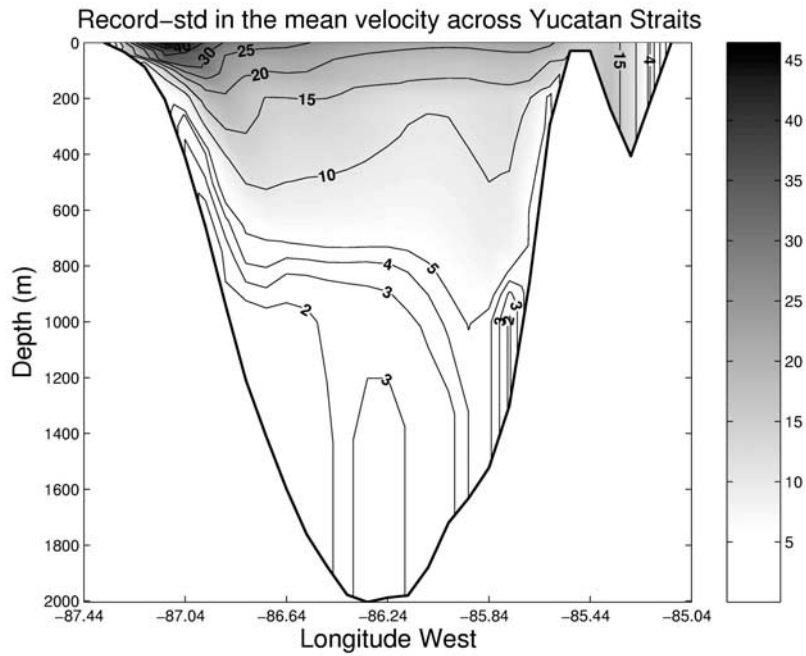


Figure 9. Deviation (in cm s^{-1}) from the mean meridional velocity across the Yucatan Straits (21.83°N , 87.44°W – 85.04°W) that is shown in Figure 8.

isotherm is similar, ranging between 100–200 m. At 500 m, the temperature both in the model and in the observations is less than 5°C . The subsurface eddy salinity maximum is located at 100–120 m depth in the model and at about 150–

200 m depth in the observations. Similarly, the 35 ppt salinity occurs at 200–300 m depth in the model, much shallower than by *Elliott* [1982, Figure 1]. Finally, *Cooper et al.* [1990, Figure 2b] late summer eddy (shed in August)

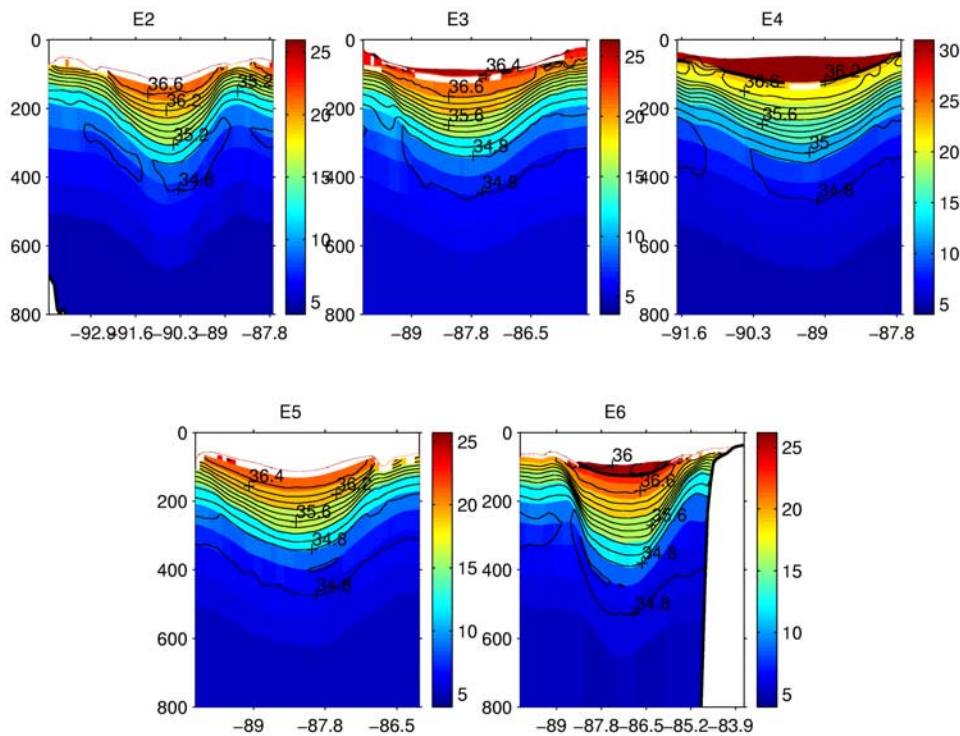


Figure 10. Temperature and salinity across a longitudinal section of each Loop Current eddy after it has been shed. The eddies are labeled according to Figure 1. The horizontal axis is in degrees west, and the vertical axis is depth in meters. Contour intervals are common for all plots, but each plot has a different color axis.

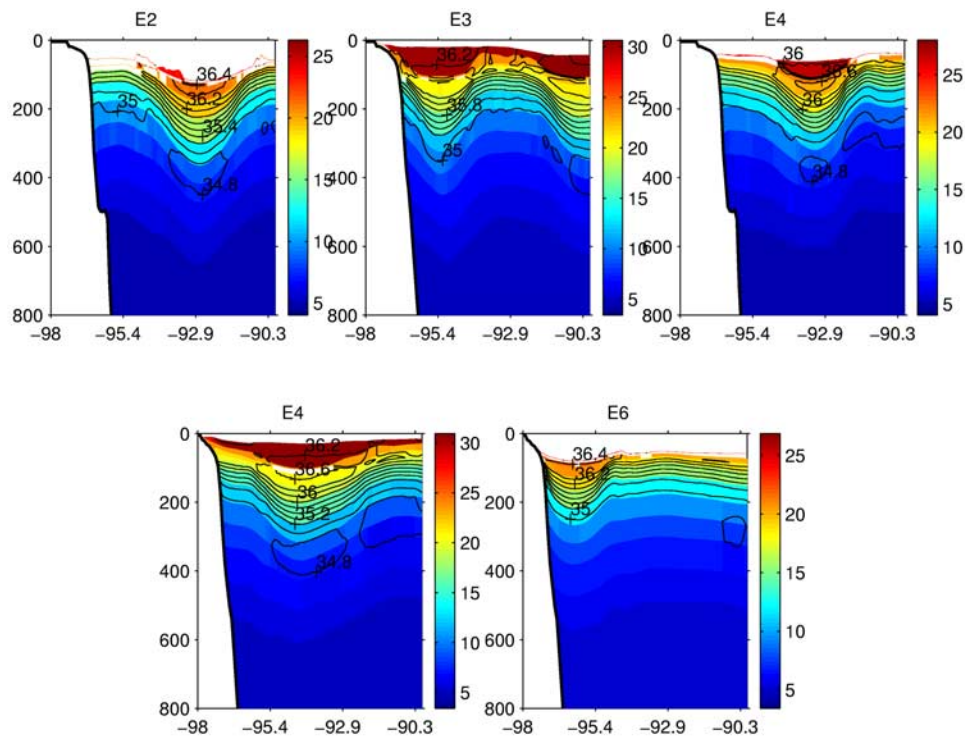


Figure 11. Similar to Figure 10 but for Loop Current eddies when they reach the western Gulf of Mexico coast. Again, the eddies are labeled according to Figure 1.

compares well with eddy E5 shed in September. The surface temperature does not differ much between the observations and the model results, but the 20°C isotherm extends between 100–220 m in the model and between 80–250 m in the observations. The temperature at 400 m is colder by about 3°C in the model than in the observations.

[40] Overall, the differences between the model eddies and the observed ones are not surprising. These are to be expected since month-to-month and year-to-year differences in weather, including large weather fronts and hurricanes, can easily induce such differences in the near-surface eddy properties.

[41] As the eddies migrate westward, their salinity and temperature signatures evolve toward those of the surroundings (Figure 11). Comparison of Figures 10 and 11 shows that when the eddies reach the western gulf coast, they have not decreased greatly in surface area. The eddies appear to freshen by about 0.2 ppt and cool by about 1°C during their lifetimes. This cooling/freshening is uniform with depth

between 150 and 300 m, over a timescale of the order of the eddy life span. The core T,S gradients with depth become $0.05^{\circ}\text{C m}^{-1}$ and 5×10^{-3} ppt m^{-1} . Eddies 1, 3, and 4 in Figure 10 maintain the salinity minimum of 34.7 ppt below 400 m, and eddies 3 and 4 maintain their subsurface salinity maximum of 36.6 ppt on the 22.5°C isotherm.

[42] Detailed characteristics for each anticyclone at formation and at the time that it reaches the western Gulf of Mexico are given in Table 4. The vertical extent of the Loop Current eddies is known from observations to be between 800 and 900 m. To investigate the model eddy vertical structure, sections of relative vorticity of newly formed Loop Current eddies at 3 different depths (50 m, 800 m, and 1500 m) are shown in Figure 12. At 800 m, the vorticity is similar to that at the surface, while much reduced in amplitude and width. At that depth, positive vorticity (cyclones) appear near the edges of the eddy. At 1500 m, a cyclonic eddy of smaller diameter is found below the anticyclone above [as

Table 4. Cyclonic Eddy Characteristics From the Present Model and Two Sets of Observations

Eddy	Surf. Temp. at Birth	Surf. Temp. Later	Surf. Saln. at Birth	Surf. Saln. Later	Max. Saln.	Max. Saln. Depth	Min. Saln.	Min. Saln. Depth
1	—	—	—	—	—	—	—	—
2	24	22	36.05	36.25	36.7	160	34.8	400
3	25.5	30	35.86	36.15	36.74	150	34.7	400
4	31	24.2	35.94	36.08	36.7	135	34.68	414
5	24	30	36.03	36.06	36.71	125	34.57	399
6	25.8	25.8	36	35.95	36.71	129	34.6	445

^aDepths are in meters.

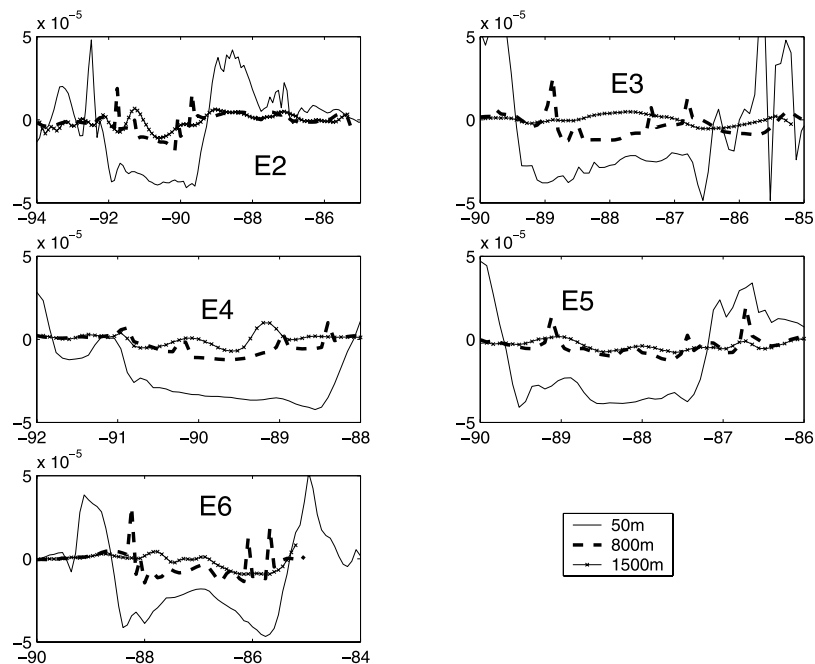


Figure 12. Vorticity (s^{-1}) across a zonal section of each newly formed eddy (eddies numbered 2–6 in Table 1 and Figure 1), at 50 m (thin line), 800 m (dashed line) and 1500 m (crossed line) depth. Horizontal axes are longitudinal sections.

in other numerical studies by *Hurlburt and Thompson* [1980], *Sturges et al.* [1993], and *Welsh and Inoue* [2000]. The model deep cyclone always survives longer than the anticyclone.

[43] As the eddies migrate west and approach the western gulf coast, the influence of the steep slope in the lower layer

becomes apparent (Figure 13). Comparison of Figures 12 and 13 shows that the eddies maintain the magnitude of their relative vorticity in each layer as well as their coherence down to 800 m, in agreement with the findings of *Hamilton et al.* [1999]. Below 800 m, there is large (usually positive) vorticity at the slope (e.g., left side of

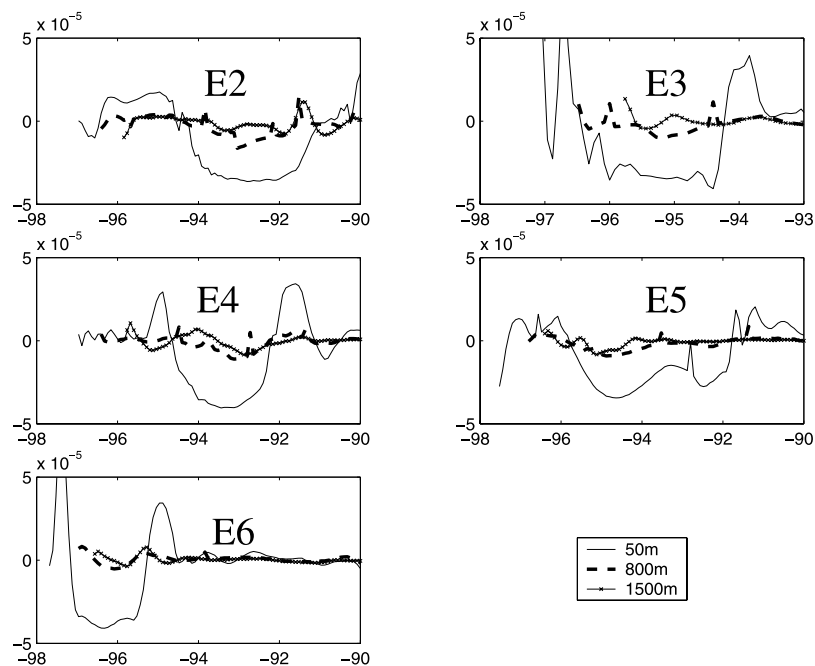


Figure 13. Same as in Figure 12, but when each eddy is close to the western boundary and at 50 m (thin line), 800 m (dashed line), and 1500 m (crossed line) depth.

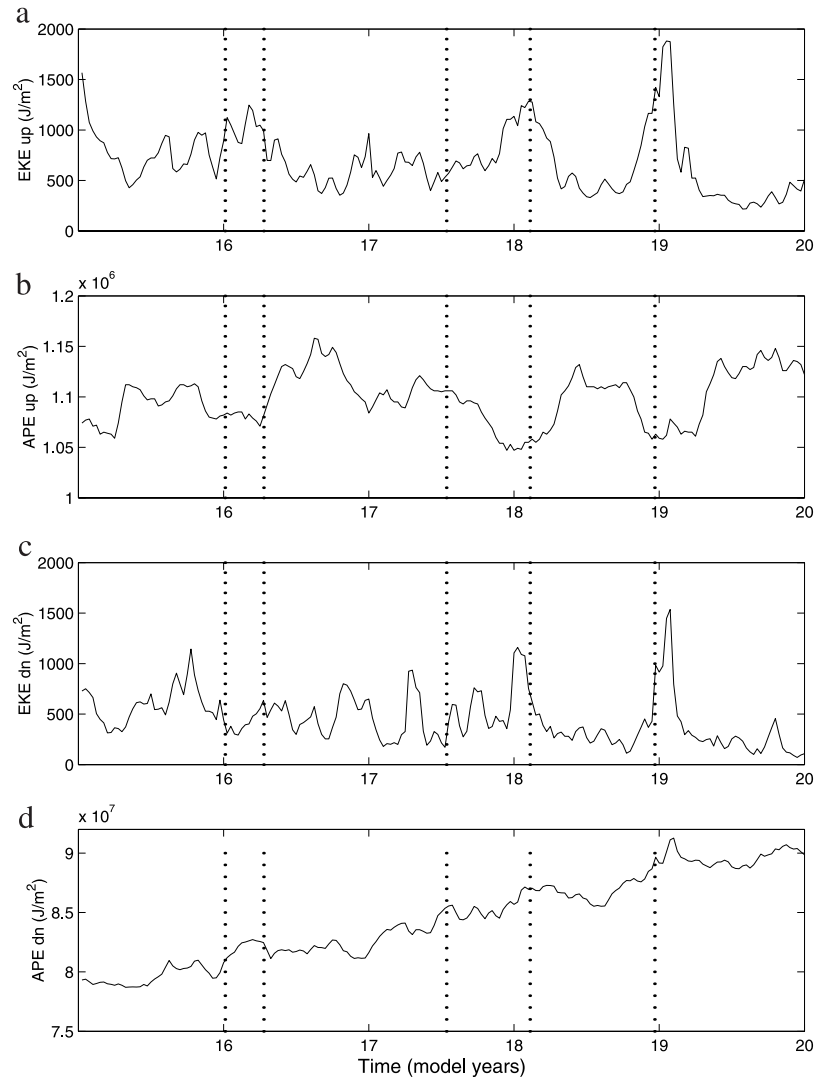


Figure 14. Time series of the area-integrated eddy kinetic energy (EKE) and available potential energy (APE): (a) and (b) the energetics in the layer above 900 m and (c) and (d) the energetics in the layer below 900 m. The dotted lines correspond to eddy shedding events (eddies E2–E6). The horizontal axis is time in model years.

the plot in Figure 12 for eddies E3–E6). This positive (cyclonic) vorticity implies that a deep cyclone exists at 1500 m and its interaction with the coast gives rise to a northward boundary current. More detailed description of the flow at 1500 m is given later in section 4.4. Eddy E2 in Figure 13 is not near the coast yet (May of year 17 in Figure 1) and later on merges with E3.

4.3. Energetics

[44] Numerical simulations allow for the study of mean and eddy kinetic energy and the available eddy potential energy and the conversions between them. Conversion between mean and eddy kinetic energy is identified with barotropic instability whereas conversion between potential and eddy kinetic energy implies baroclinic instability [Bleck, 1985]. Investigating the energy conversion mechanism in the present model simulation provides insight into the Loop Current evolution and into the formation and detachment of the anticyclonic eddies.

[45] Following Bleck [1985] and Chassignet and Boudra [1988], the area averaged eddy kinetic energy (EKE) and the available eddy potential energy (APE) are respectively:

$$\text{EKE} = \frac{1}{A} \int_A \int_{\text{bot}}^{\text{top}} \frac{\overline{(u'^2 + v'^2)}}{2} h \, d\rho \, dA \quad (2)$$

$$\text{APE} = \frac{g}{A} \int_A \frac{(d - \hat{d})^2}{2} \delta\alpha \, dA, \quad (3)$$

where the overbar denotes time average, primed quantities are the eddy velocities (i.e., the deviations from the mass-weighted time averages), h is the layer thickness, and d the interface depth. Hatted quantities represent area averages. A is the total basin area (adjusted to account for topography), ρ the layer density, and $\delta\alpha$ the specific volume jump across each layer interface.

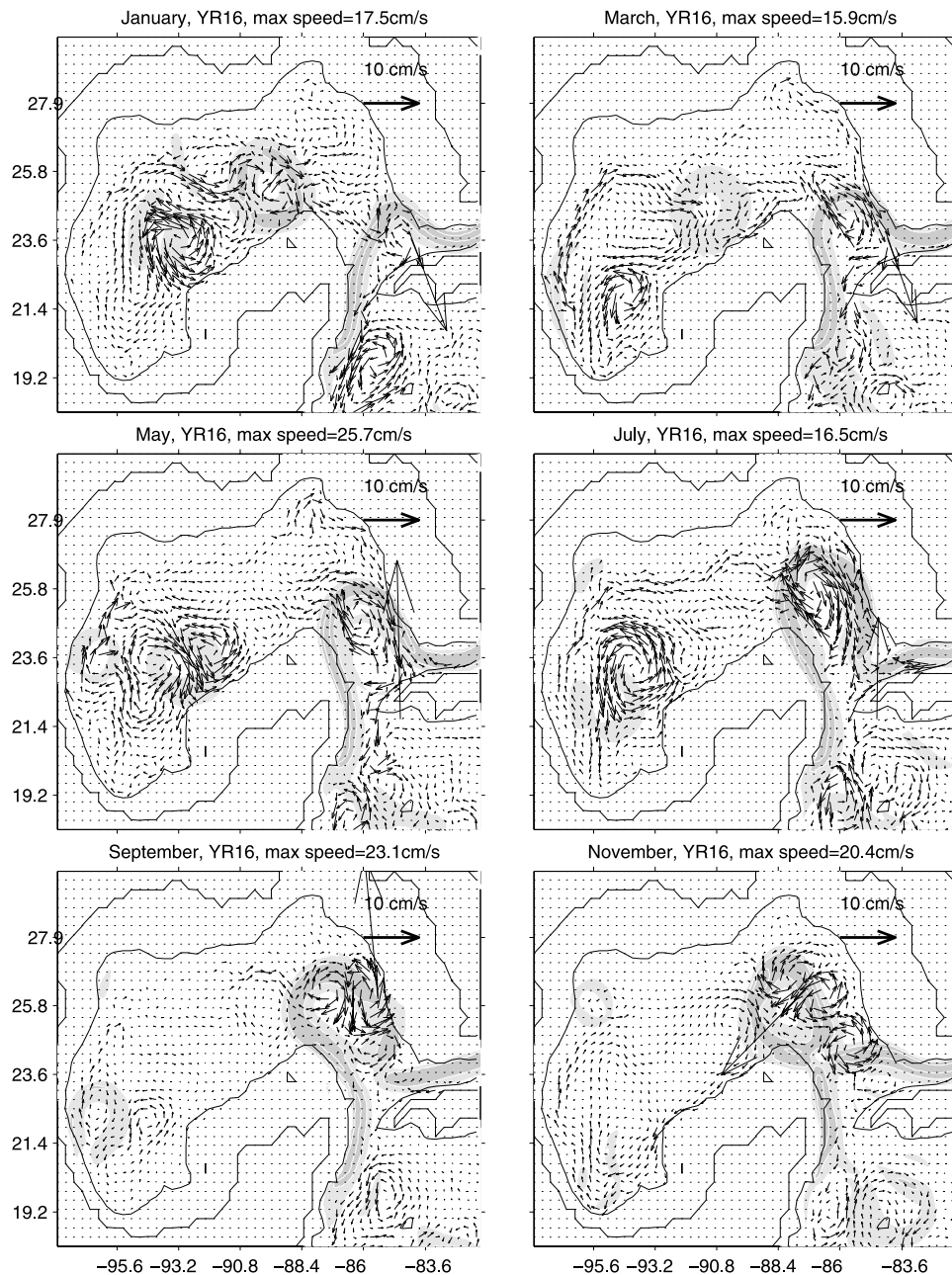


Figure 15. Velocity field at 1500 m (in cm s^{-1}) every 2 months in analogy to Figure 1. Vectors are plotted every $1/6^\circ$. The max speed shown at the heading of each plot is in cm s^{-1} and corresponds to the largest arrow in each plot. The position of Loop Current and Loop Current eddy at 50 m is indicated with gray shading. The 1 m and the 1000 m isobaths are also denoted.

[46] During the time leading to eddy shedding while the Loop Current frontal boundary advances farther into the Gulf of Mexico, the eddy kinetic energy of the upper layer (down to 900 m) increases (Figure 14a) and the eddy potential energy decreases (Figure 14b) implying that baroclinic instability plays an important role in the formation and detachment of the Loop Current anticyclones. The correlation between the two time series is -0.7 .

[47] During the same time, the eddy kinetic energy below 900 m (Figure 14c) also increases indicating that Loop Current eddy shedding is associated with eddy generation below the Loop Current. The correlation between the upper and lower layer eddy kinetic energy is 0.65. However, in the

deeper layer, the potential energy does not appear to be the source of the eddy variability (Figure 14d). It is concluded that the deep eddies develop because of shear stress forcing from the upper layer.

4.4. Currents at and Below 1500 m

[48] The discussion in the previous section suggested that the eddy activity in the deeper parts of the Gulf of Mexico is forced from the top. The model flow at 1500 m is now described.

[49] At 1500 m (Figure 15), the strongest currents in the model are associated with the Loop Current or with Loop Current eddies at the surface (shaded regions). In the eastern

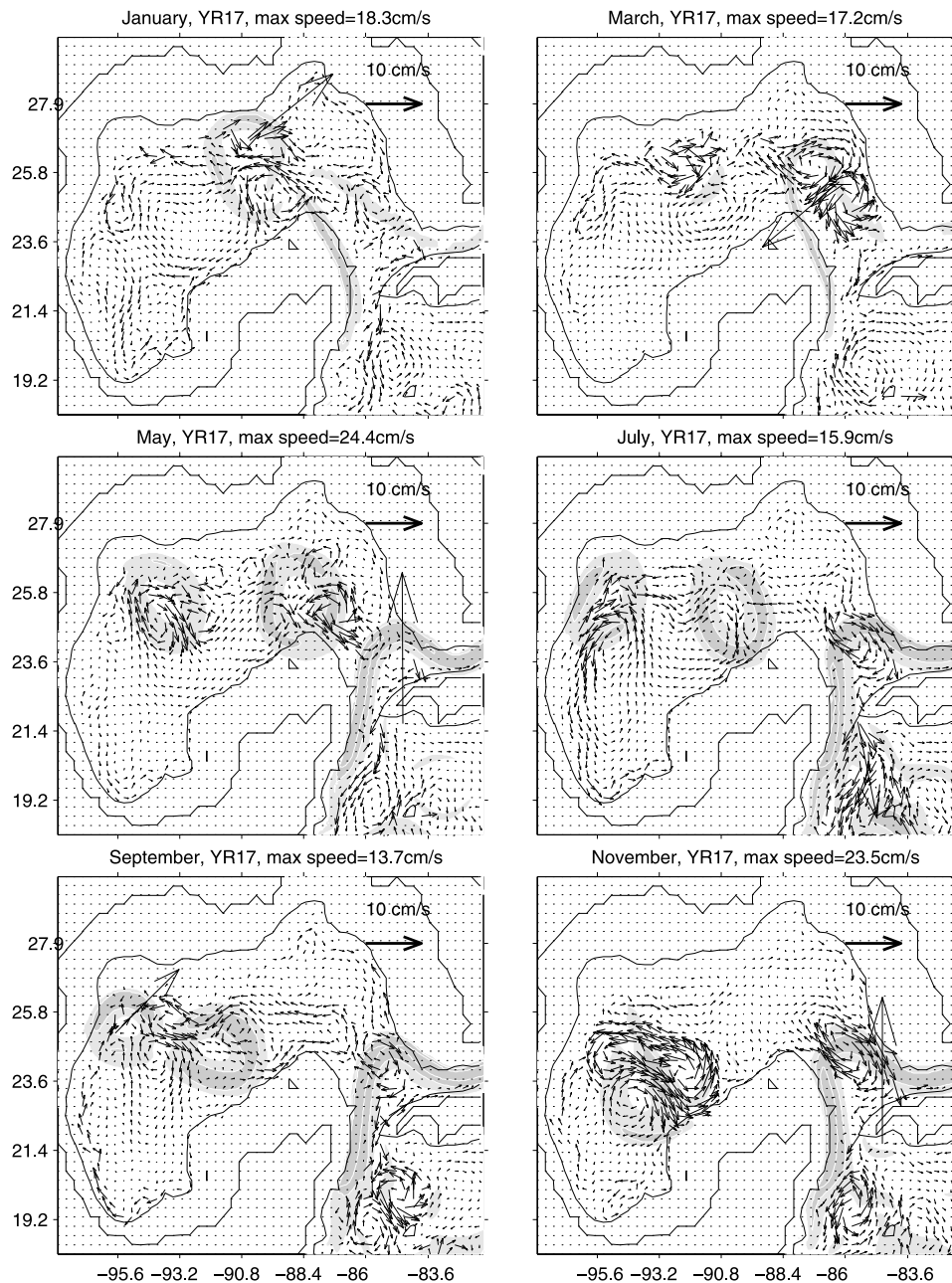


Figure 15. (continued)

gulf, a strong anticyclonic circulation of about 15 cm s^{-1} is found between the Campeche Bank and the southwest Florida Slope (as in Figure 15: March–July of year 16, July of year 17, January of year 18, September–November of year 18, May–November of year 19, and July November of year 20). However, in the few months preceding a shedding (Table 1), these deep anticyclones break up and form pairs of anticyclones (on the north side of the gulf) and cyclones (at the entrance to the gulf) (as in Figure 15: November of year 16, March of year 17, March of year 18, and January of year 19 for weak anticyclone, and November of year 20 for weak cyclone confined near the Florida tip). It appears that the deep anticyclone-cyclone pairs form when the Loop Current boundary becomes unstable and an eddy

is shed. In these pairs, the cyclones are more energetic, with speeds of $18\text{--}19 \text{ cm s}^{-1}$. A similar flow pattern (although weaker) was found in simulations by *Sturges et al.* [1993] and more recently in simulations by *Welsh and Inoue* [2000].

[50] In the present model, deep anticyclone diameters range between 250 and 500 km and deep cyclone diameters between 130 and 500 km. The cyclones move at speeds that range between 0.4 and 7.3 km d^{-1} , with a mean speed of 3.8 km d^{-1} , and live 9 months on average (7–11 months). The anticyclones have translational speeds between $0.9\text{--}5.4 \text{ km d}^{-1}$ with a mean speed of 2.1 km d^{-1} , and have a slightly shorter lifetime than the cyclones. These results are in agreement with those of *Welsh and Inoue* [2000], who

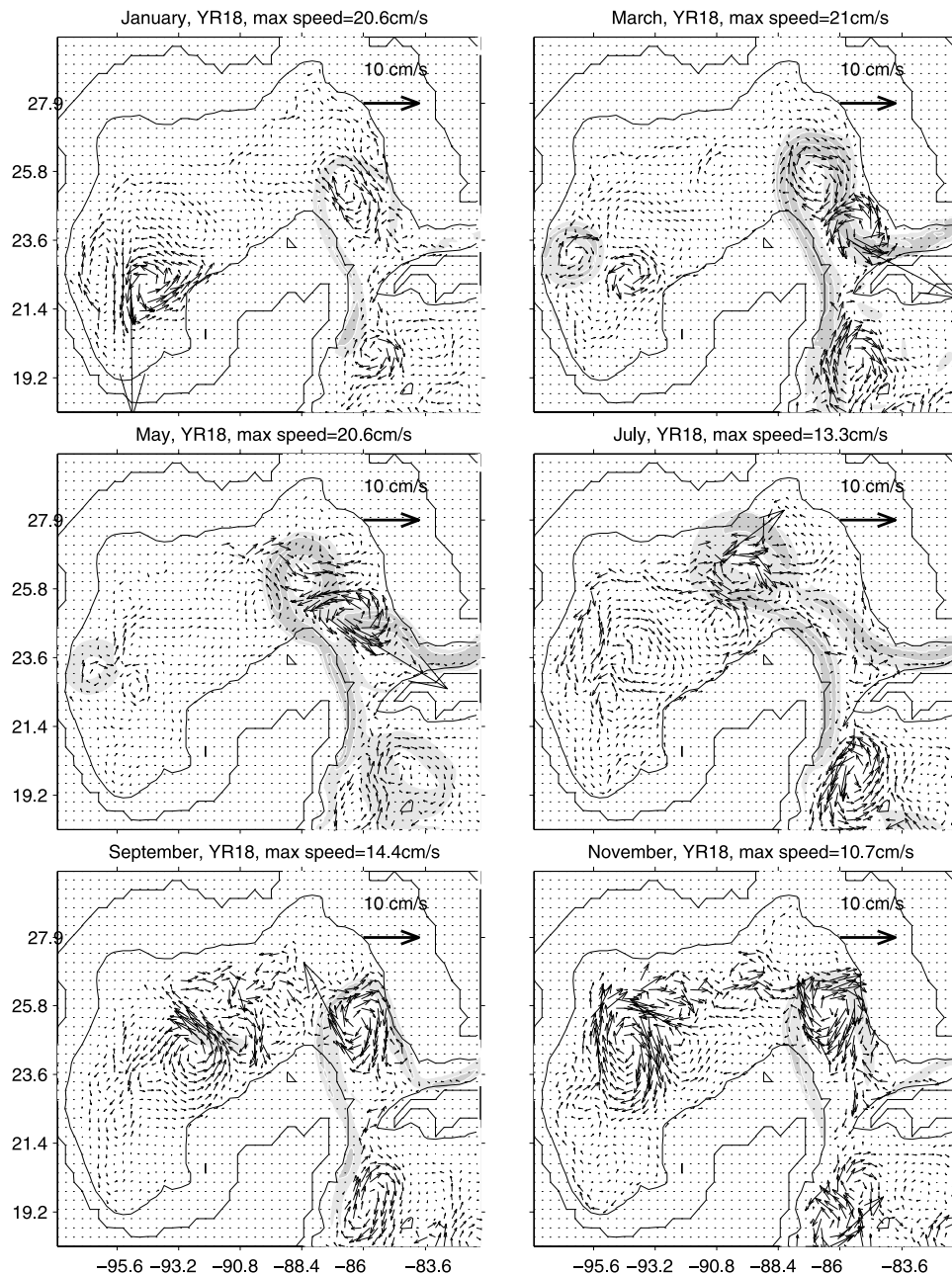


Figure 15. (continued)

found orbital speeds of the deep eddies up to $10\text{--}21\text{ cm s}^{-1}$, diameters around 270 km , translation speeds of 3.7 km d^{-1} , and life spans of around 300 days.

[51] In the western gulf, the surface anticyclonic eddies that were originally shed from the Loop Current are often associated with cyclones at 1500 m , as in Figure 15: in January and July of year 16, November of year 17, January and November of year 18, March and November of year 19, and July of year 20. Most of the deep cyclonic eddies associated with the Loop Current anticyclones expire in Campeche Bay, while the surface Loop Current eddy splits and moves north along the coast. As described in section 4.2, the cyclonic vorticity near the deep slope of the western Gulf of Mexico results from the disintegrating cyclones (e.g., March and July–November of year 16,

September–November of year 17, January of year 18, and November of year 19). The southward boundary currents associated with these features are not permanent and are only occasionally strong (November of year 17) in Figure 15.

[52] Conservation of potential vorticity arguments may help explain why the deep cyclones tend to outlive their deep anticyclonic partners. Comparison of Figures 12 and 13 shows that the relative vorticity of the surface layers changes little in time. Assuming that the β -induced vorticity is small compared to the relative vorticity, then the relative vorticity of the deep eddies must increase when the deep cyclone–anticyclone pair encounters the western gulf slope. The deep anticyclone (with negative relative vorticity) spins down while the cyclone (with positive relative vorticity) survives. Such a heuristic argument

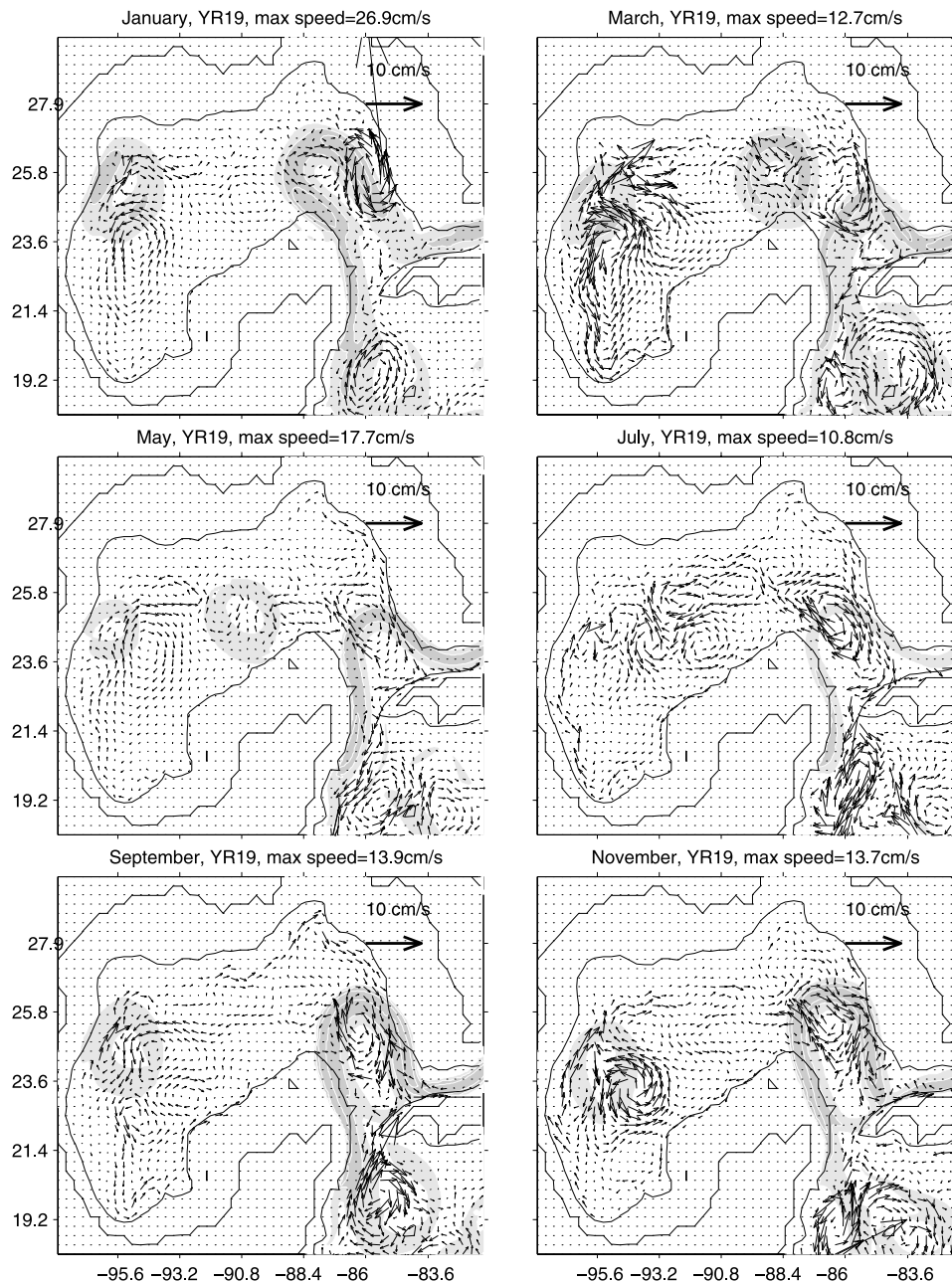


Figure 15. (continued)

should however be further investigated using idealized model configurations.

[53] Off the West Florida Slope, the deep circulation is dominated by the eddies. The strongest velocities of about 20 cm s^{-1} (in agreement with observations by *Hamilton* [1990]) are associated with the anticyclones or cyclones when the Loop Current is about to shed an eddy. At other times, even after the shedding, the circulation close to the straits is weaker (Figure 15). *Hamilton* [1990] observed mean currents off the central-west Florida slope of 2 cm s^{-1} (in good agreement with those found in the model) and 3 cm s^{-1} farther to the north and east (double the current speed found in the model).

[54] The spectrum of the flow at 1500 m shows that in the eastern gulf the variability ranges from 5 to 10 months, in

the central gulf from 15 to 20 months, and in the western gulf from 5 to 10 months. The variability in the western gulf is attributed to the Loop Current eddies and is consistent with topographic Rossby waves created from their interaction with the boundary (as observed by *Hamilton* [1999] and found in numerical simulations of the gulf by *Oey* [1996]). In a recent paper, *Oey and Lee* [2002] identified eddy kinetic energy variability with periods longer than 20 days with topographic Rossby waves. In the present model (Figure 16) as well 90% of the deep eddy kinetic energy variability is contained within 55–381 days.

[55] Figure 17 shows the time-mean velocity field across several zonal sections in the Gulf of Mexico. Below 1500 m, the circulation is usually vertically coherent in the middle sections of the gulf. Variability in the vertical exists mostly

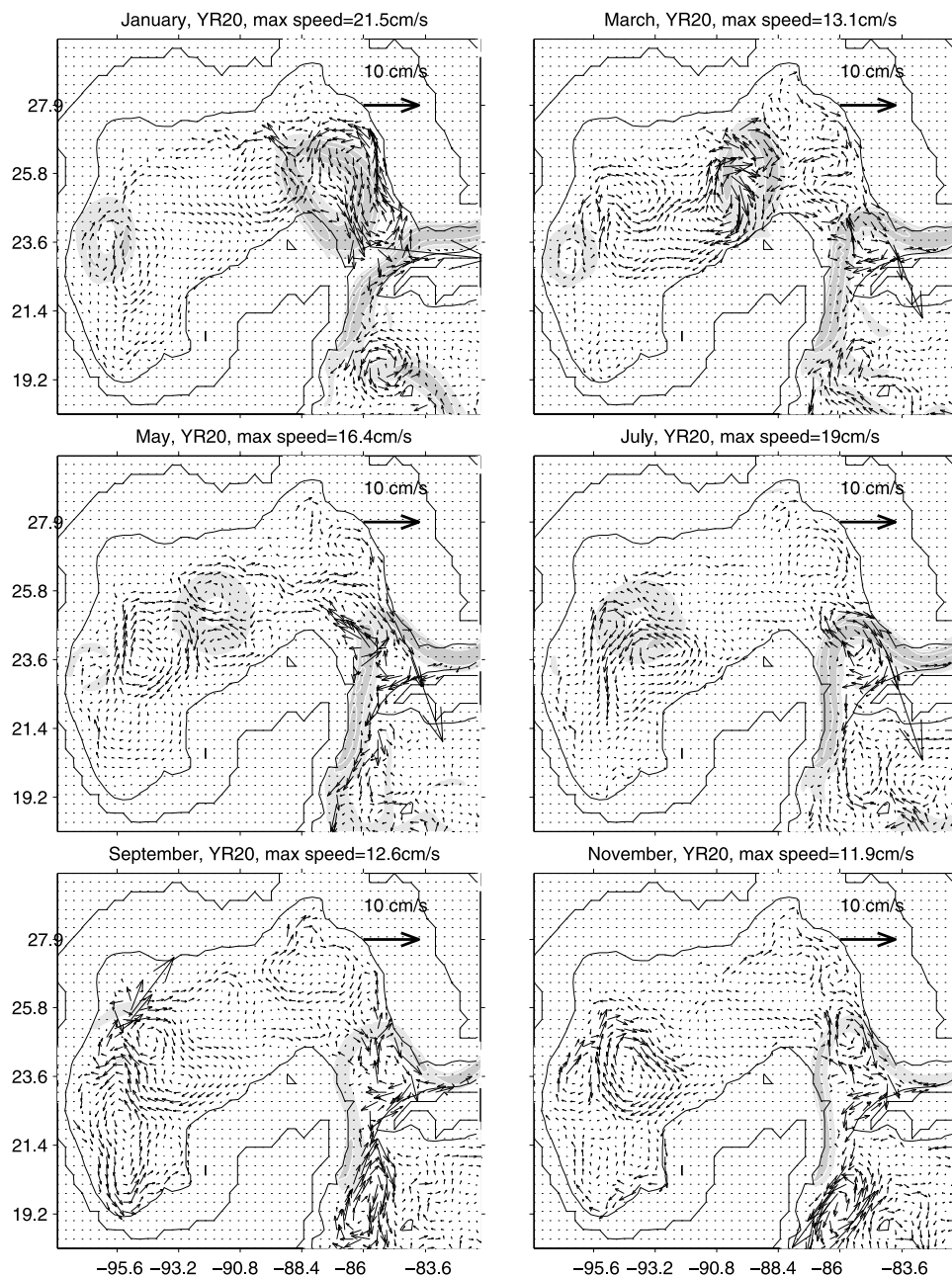


Figure 15. (continued)

close to the boundaries. At 27.3°N (essentially the DeSoto Canyon area: around $85.5^{\circ}\text{--}87^{\circ}\text{W}$), the flow is to the north at 1500 m, while the flow at 2000 m is stronger and directed to the south-southwest. At 25.9°N , the flow is stronger at 2000 m than at 1500 m close to the West Florida Slope (at 85.27°W). Across 24.4°N and 23°N , the flow in the eastern Gulf of Mexico is in opposite directions at 1500 m and 2000 m. Significant bottom intensification (on the order of 10 cm s^{-1} relative to the currents at 50 m) is found in Campeche Bay (21.5°N section between $93^{\circ}\text{--}96^{\circ}\text{W}$), the area where the deep cyclones expire. *Hamilton* [1990] found currents as large as $12\text{--}15\text{ cm s}^{-1}$ at several deep mooring stations. The model shows velocities of the same magnitude at the same locations and even larger ones at locations northeast of the Campeche Bay. Topographic

control of fast and transient features (eddies) below 1500 m could explain the bottom intensification near boundaries, but this can only be further investigated via detailed idealized studies.

5. Summary and Conclusions

[56] The surface and deep circulation in the Gulf of Mexico has been studied with the aid of a fine mesh numerical simulation of the North and equatorial Atlantic Ocean. The model domain is much larger than the specific area of interest (i.e., the Gulf of Mexico), and the inflow/outflow from the Yucatan and/or the Florida Straits are not prescribed but rather result from the model dynamics over the whole North Atlantic basin. This is the first study that

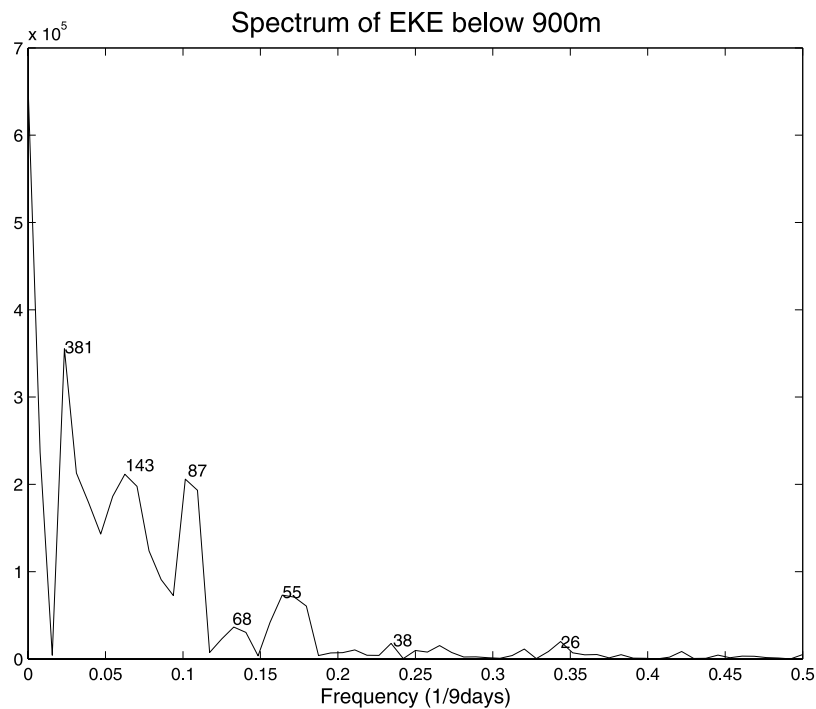


Figure 16. Spectrum of the area-integrated eddy kinetic energy below 900 m. The actual time series is shown in Figure 13c. The numbers denote the period of each spectral peak in days.

aims to analyze the Gulf of Mexico circulation from within a North Atlantic simulation. The need for boundary conditions far away from the Gulf of Mexico was first pointed out by *Sturges* [1992], who suggested that the plethora of spectral peaks in the eddy shedding spectrum was the result of frequency interactions, some of remote origin such as the North Brazil Current and the Gulf Stream. Consequently, *Sturges et al.* [1993] placed the outside model boundary at the Mid-Atlantic Ridge, and *Oey* [1996] demonstrated that setting the boundary farther south at the Caribbean rather than at the Yucatan Straits allowed for a better representation of the Gulf of Mexico circulation. *Ezer et al.* [2003] prescribed open boundaries sufficiently removed from the Gulf of Mexico to allow for a free dynamical interaction between the Caribbean Sea and the gulf through the Yucatan Channel. Our modeled eddy shedding frequency consists of multiple spectral peaks which, as by *Sturges* [1992], can be attributed to interactions of the natural shedding frequency with the frequencies of variability of other oceanographic forcing fields, such as the Yucatan Channel inflow, the Florida Current and North Brazil Current variability, as well as the synoptic meteorological forcing variability.

[57] Good agreement with observations was found regarding eddy shedding frequency and the Loop Current eddy characteristics. Eddy shedding in the model occurred typically every 8–9 months and produced anticyclones with diameters ranging from 140 to 500 km with a mean of 300 km, an average translation speed of 3 m d^{-1} , and an average lifetime of 1 year. All major eddy characteristics such as the westward propagation path, the vertical extent, and the temperature and salinity structure agree very well with observations. The anticyclones retain their shape and most of their surface hydrographic features as they translate west. When they reach the western gulf coast, they feel the

influence of the steep topography in that region, which slowly dissipates the eddies.

[58] Surface cyclonic eddies exist everywhere in the gulf but are mostly concentrated in three regions: off the southwestern Florida shelf, around the Loop Current boundary as the Loop Current extends northward, and in the western Campeche Bay. They live half as long as the Loop Current eddies, but propagate 2 to 3 times as fast. Their orbital speeds are much less than those of the Loop Current eddies. However, despite its high resolution, the model is unable to describe adequately the smaller size, less than 10 km, cyclones which are very energetic and ubiquitous in the gulf.

[59] Not surprisingly, the model surface circulation in the eastern Gulf of Mexico is dominated by the transient Loop Current as it penetrates northward, the Loop Current eddies, and some vigorous cyclones that develop in the region. Significant correlation is found between the Loop Current eddy shedding and strong northward currents off southwestern Florida. Area-averaged energetics in the gulf show that the main mechanism for eddy shedding is the baroclinic transfer of eddy potential to eddy kinetic energy. The western Gulf of Mexico surface circulation is dominated by mesoscale features such as translating Loop Current eddies and cyclones.

[60] Given the good agreement of the modeled fields with the observed Gulf of Mexico circulation, we expanded our analysis to the deep circulation where few observations are available (with exceptions such as the recent *Bunge et al.* [2002] mooring experiment). The deep circulation in the Gulf of Mexico (below the Yucatan Straits sill depth) is dominated by families of anticyclones and cyclones that are created when the Loop Current sheds eddies. These features move westward, with cyclones outliving the anticyclones,

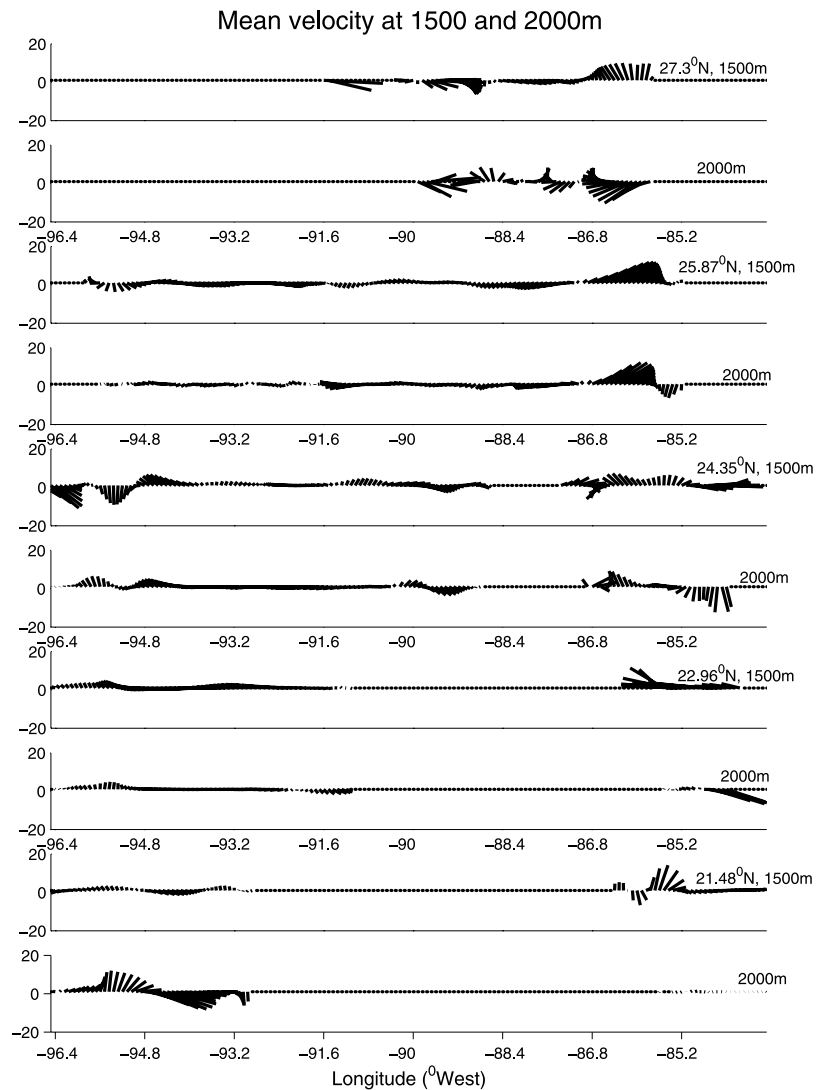


Figure 17. Five pairs of east-west cross sections of the time-mean velocity field at (top) 1500 m and (bottom) 2000 m.

since conservation of potential vorticity near a western sloping boundary suggests that cyclones should be favored over anticyclones. The deep cyclones accompany the Loop Current anticyclones to the western gulf coast, where the surface anticyclones move north and the deep cyclones move into the Campeche Bay area and quickly dissipate there. The deep cyclones are as large as the surface anticyclones and have nearly equal lifetimes. Strong deep currents off the West Florida Shelf (of 20 cm s^{-1}) are associated with transient pairs (cyclones-anticyclones) arising from Loop Current eddy shedding. The western gulf shows strong currents close to the topography of about $10\text{--}15 \text{ cm s}^{-1}$ on average. Bottom intensification occurs especially close to the lateral boundaries (slopes).

[61] The surface circulation in the Gulf of Mexico in the present simulation, even though it is forced by mean monthly wind fields, is quite realistic. It therefore leads us to the conclusion that basin-scale (North Atlantic) numerical simulations with sufficiently high resolution are able to reproduce the large-scale as well as the mesoscale variabil-

ity of intricate subbasins such as the Gulf of Mexico. Several questions remain unanswered, such as what is the role of daily/interannual forcing, how do the eddies interact among themselves and with the topography, and what are the mechanisms that describe the pairing and propagation of the eddies.

[62] **Acknowledgments.** This research was supported by MMS study contract 01-99-CT-31027 and NSF grants OCE-9531852 and ATM-9905210. Computations were performed on the Department of Defense (DoD) computers at the Stennis Space Center under a challenge grant from the DoD High Performance Computer Modernization Office. The authors thank Zulema Garraffo for her assistance with the model outputs and Linda Smith for her careful editing of the manuscript.

References

- Bleck, R. (1985), On the conversion between mean and eddy components of potential and kinetic energy in isentropic and isopycnic coordinates, *Dyn. Atmos. Oceans*, *9*, 17–37.
- Bleck, R., and Chassignet, E. P. (1994), Simulating the oceanic circulation with isopycnic coordinate models, in *The Oceans: Physiochemical Dynamics and Resources*, edited by S. K. Majumdar et al., pp. 17–39, Penn. Acad. of Sci., Harrisburg.

- Bleck, R., C. Rooth, D. Hu, and L. T. Smith (1992), Salinity-driven transients in a wind- and thermohaline-forced isopycnic coordinate model of the North Atlantic, *J. Phys. Oceanogr.*, *22*, 1486–1505.
- Bracco, A., E. P. Chassignet, Z. D. Garraffo, and A. Provenzale (2003), Lagrangian velocity distributions in a high-resolution numerical simulation of the North Atlantic, *J. Oceanos Atmos. Technol.*, *20*, 1212–1220.
- Bunge, L., J. Ochoa, A. Badan, J. Candela, and J. Sheinbaum (2002), Deep flows in the Yucatan Channel and their relation to changes in the Loop Current extension, *J. Geophys. Res.*, *107*(C12), 3233, doi:10.1029/2001JC001256.
- Chassignet, E. P., and D. B. Boudra (1988), Dynamics of Agulhas retroflexion and ring formation in a numerical model. part II. Energetics and ring formation, *J. Phys. Oceanogr.*, *18*, 304–319.
- Chassignet, E. P., and Z. D. Garraffo (2001), Viscosity parameterization and the Gulf Stream separation, in “*From Stirring to Mixing in a Stratified Ocean*,” edited by P. Muller and D. Henderson, pp. 37–41, Univ. of Hawaii, Honolulu.
- Chassignet, E. P., L. T. Smith, R. Bleck, and F. O. Bryan (1996), A model comparison: Numerical simulations of the North and equatorial Atlantic oceanic circulation in depth and isopycnic coordinates, *J. Phys. Oceanogr.*, *26*, 1849–1867.
- Cochrane, J. D. (1969), Separation of an anticyclone and subsequent development in the Loop Current, in *Contributions on the Physical Oceanography of the Gulf of Mexico*, vol. II, edited by L. R. A. Capurro and J. L. Reid, pp. 3–51, Gulf, Houston, Tex.
- Cooper, C., G. Z. Forristall, and T. M. Joyce (1990), Velocity and hydrographic structure of two Gulf of Mexico warm-core rings, *J. Geophys. Res.*, *95*, 1663–1679.
- Cushman-Roisin, B., E. P. Chassignet, and B. Tang (1990), Westward motion of mesoscale eddies, *J. Phys. Oceanogr.*, *20*, 758–768.
- da Silva, A. M., C. C. Young, and S. Levitus (1994), Atlas of surface marine data 1994, technical report, Natl. Oceanic and Atmos. Admin., Silver Spring, Md.
- Dietrich, D. E., C. A. Lin, and A. Mestas-Nunez (1997), A high resolution numerical study of Gulf of Mexico fronts and eddies, *Meteorol. Atmos. Phys.*, *64*, 187–201.
- Elliott, B. A. (1982), Anticyclonic rings in the Gulf of Mexico, *J. Phys. Oceanogr.*, *12*, 1292–1309.
- Ezer, T., L.-Y. Oey, H.-C. Lee, and W. Sturges (2003), The variability of currents in the Yucatan Channel: Analysis of results from a numerical ocean model, *J. Geophys. Res.*, *108*(C1), 3012, doi:10.1029/2002JC001509.
- Fratantoni, P. S., T. N. Lee, and G. P. Podesta (1998), The influence of Loop Current perturbations on the formation and evolution of Tortugas eddies in the southern Straits of Florida, *J. Geophys. Res.*, *103*, 24,759–24,779.
- Garraffo, Z. D., A. J. Mariano, A. Griffa, C. Veneziani, and E. P. Chassignet (2001), Lagrangian data in a high-resolution numerical simulation of the North Atlantic. I. Comparison with in situ drifter data, *J. Mar. Syst.*, *29*, 157–176.
- Garraffo, Z. D., W. E. Johns, E. P. Chassignet, and G. J. Goni (2003), North Brazil Current rings and transport of southern waters in a high resolution numerical simulation of the North Atlantic, in *Interhemispheric Water Exchange in the Atlantic Ocean*, edited by P. Malanotte-Rizzoli and G. J. Goni, Elsevier Oceanogr. Ser., in press.
- Goni, G. J., and W. E. Johns (2001), A census of North Brazil current rings observed from TOPEX/Poseidon altimetry: 1992–1998, *Geophys. Res. Lett.*, *28*, 1–4.
- Hamilton, P. (1990), Deep currents in the Gulf of Mexico, *J. Phys. Oceanogr.*, *20*, 1087–1104.
- Hamilton, P., and A. L. Fernandez (2001), Observations of high speed deep currents in the northern Gulf of Mexico, *Geophys. Res. Lett.*, *28*, 2867–2870.
- Hamilton, P., G. S. Fargion, and D. C. Biggs (1999), Loop Current eddy paths in the western Gulf of Mexico, *J. Phys. Oceanogr.*, *29*, 1180–1207.
- Hofmann, E. E., and S. J. Worley (1986), An investigation of the circulation of the Gulf of Mexico, *J. Geophys. Res.*, *91*, 14,221–14,236.
- Hurlburt, H. E., and J. D. Thompson (1980), A numerical study of Loop Current intrusions and eddy shedding, *J. Phys. Oceanogr.*, *10*, 1611–1651.
- Johns, W. E., S. L. Garzoli, and G. J. Goni (2003), Cross-gyre watermass transport by North Brazil Current Rings, in *Interhemispheric Water Exchange in the Atlantic Ocean*, edited by P. Malanotte-Rizzoli and G. J. Goni, Elsevier Oceanogr. Ser., in press.
- Larsen, J. C. (1992), Transport and heat flux of the Florida Current at 27° derived from cross-stream voltages and profiling data: Theory and observations, *Philos. Trans. R. Soc. London*, *338*, 169–236.
- Lee, T. N., K. Leaman, E. Williams, T. Berger, and L. Atkinson (1995), Florida current meanders and gyre formation in the southern straits of Florida, *J. Geophys. Res.*, *100*, 8607–8620.
- Levitus, S. (1982), Climatological atlas of the world ocean, *NOAA Prof. Pap. 13*, U.S. Govt. Print. Off., Washington, D. C.
- Maul, G. A., and F. M. Vukovich (1993), The relationship between variations in the Gulf of Mexico Loop Current and Straits of Florida volume transport, *J. Phys. Oceanogr.*, *23*, 785–796.
- Maul, G. A., D. A. Mayer, and S. R. Baig (1985), Comparisons between a continuous 3-year current-meter observation at the sill of the Yucatan Strait, satellite measurements of the Gulf Loop Current area and regional sea level, *J. Geophys. Res.*, *90*, 9089–9096.
- Molinari, R. L., and D. A. Mayer (1982), Current meter observations of the continental slope and two sites in the eastern Gulf of Mexico, *J. Phys. Oceanogr.*, *12*, 1480–1492.
- Molinari, R. L., and J. Morrison (1988), The separation of the Yucatan Current from the Campeche Bank and the intrusion of the Loop Current into the Gulf of Mexico, *J. Geophys. Res.*, *93*, 10,645–10,654.
- Oey, L. Y. (1996), Simulation of mesoscale variability in the Gulf of Mexico: Sensitivity studies, comparison with observations, and trapped wave propagation, *J. Phys. Oceanogr.*, *26*, 145–175.
- Oey, L. Y., and H. C. Lee (2002), Deep eddy energy and topographic Rossby waves in the Gulf of Mexico, *J. Phys. Oceanogr.*, *32*, 3499–3527.
- Özgökmen, T., E. P. Chassignet, and A. Paiva (1997), Impact of wind forcing, bottom topography, and inertia on mid-latitude jet separation in a quasi-geostrophic model, *J. Phys. Oceanogr.*, *27*, 2460–2476.
- Paiva, A. M., J. T. Hargrove, E. P. Chassignet, and R. Bleck (1999), Turbulent behavior of a fine mesh (1/12°) numerical simulation of the North Atlantic, *J. Mar. Syst.*, *21*, 307–320.
- Pichevin, T., and D. Nof (1997), The momentum imbalance paradox, *Tellus, Ser. A*, *49*, 298–319.
- Sheinbaum, J., J. Candela, A. Badan, and J. Ochoa (2002), Flow structure and transport in the Yucatan Channel, *Geophys. Res. Lett.*, *29*(3), 1040, doi:10.1029/2001GL013990.
- Sturges, W. (1992), The spectrum of Loop Current variability from gappy data, *J. Phys. Oceanogr.*, *22*, 1245–1256.
- Sturges, W. (1993), The annual cycle of the western boundary current in the Gulf of Mexico, *J. Geophys. Res.*, *98*, 18,053–18,068.
- Sturges, W. (1994), The frequency of ring separations from the Loop Current, *J. Phys. Oceanogr.*, *24*, 1647–1651.
- Sturges, W., and B. G. Hong (2000), Gulf Stream transport variability at periods of decades, *J. Phys. Oceanogr.*, *31*, 324–332.
- Sturges, W., and R. Leben (2000), Frequency of ring separations from the Loop Current in the Gulf of Mexico: A revised estimate, *J. Phys. Oceanogr.*, *30*, 1814–1819.
- Sturges, W., J. C. Evans, S. Welsh, and W. Holland (1993), Separation of warm core rings in the Gulf of Mexico, *J. Phys. Oceanogr.*, *23*, 250–268.
- Vukovich, F. M. (1986), Aspects of the behavior of cold perturbations in the eastern Gulf of Mexico: A case study, *J. Phys. Oceanogr.*, *16*, 175–188.
- Vukovich, F. M. (1988), Loop Current boundary variations, *J. Geophys. Res.*, *93*, 15,585–15,591.
- Vukovich, F. M. (1995), An updated evaluation of the Loop Current’s eddy shedding frequency, *J. Geophys. Res.*, *100*, 8655–8659.
- Vukovich, F. M., and B. W. Crissman (1986), Aspects of warm rings in the Gulf of Mexico, *J. Geophys. Res.*, *91*, 2645–2660.
- Vukovich, F. M., and G. A. Maul (1985), Cyclonic eddies in the eastern Gulf of Mexico, *J. Phys. Oceanogr.*, *15*, 105–117.
- Welsh, S. E., and M. Inoue (2000), Loop Current rings and the deep circulation in the Gulf of Mexico, *J. Geophys. Res.*, *105*, 16,951–16,959.

E. P. Chassignet, RSMAS/MPO, University of Miami, Miami, FL 33149, USA.

A. Romanou, Courant Institute of Mathematical Sciences, 251 Mercer St., NY 10012, New York University, New York, USA. (romanou@cims.nyu.edu)

W. Sturges, Department of Oceanography, Florida State University, Tallahassee, FL 32304, USA.